Advanced Drug Delivery Reviews 229 (2026) 115747

Contents lists available at ScienceDirect

Advanced Drug Delivery Reviews

journal homepage: www.elsevier.com/locate/adr

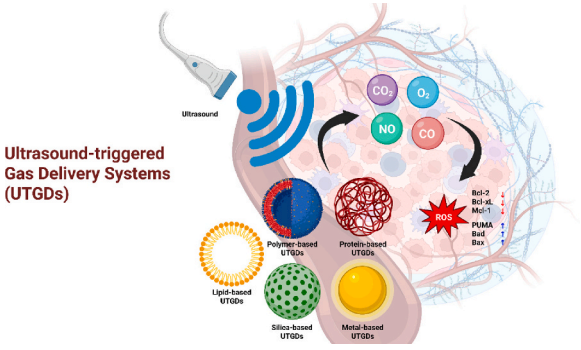
Perspectives and trends in gas delivery systems based on ultrasound responsive nanomaterials for cancer therapy☆

Jooho Moon [a,1], Hanhee Cho [c,1], Jeonghun Yu [a], Hyuncheol Kim [a,b,2,*], Kwangmeyung Kim [c,d,*]

[a] Department of Chemical and Biomolecular Engineering, Sogang University, 35 Baekbeom-ro, Mapo-gu, Seoul 04107, Republic of Korea
[b] Department of Biomedical Engineering, Sogang University, 35 Baekbeom-ro, Mapo-gu, Seoul 04107, Republic of Korea
[c] College of Pharmacy, Graduate School of Pharmaceutical Sciences, Ewha Womans University, Seoul, 03760, Republic of Korea
[d] Graduate Program in Innovative Biomaterials Convergence, Ewha Womans University, Seoul, 03760, Republic of Korea

GRAPHICAL ABSTRACT

Created in BioRender. Moon, J. (2025) https://BioRender.com/jc0643r



ARTICLE INFO

Keywords:
Ultrasound
Gas therapy
Targeted delivery
Cancer
Controlled release

ABSTRACT

Gas-based therapeutic strategies (e.g., nitric oxide and carbon dioxide delivery) have shown promising potential for modulating the tumor microenvironment and enhancing anticancer efficacy. However, their clinical translation is limited by their poor spatiotemporal control, systemic toxicity, and limited tumor selectivity. As a powerful alternative, nanomaterial-based gas delivery systems offer improved stability, targeted accumulation, and programmable release in response to tumor-specific stimuli. Among various triggering methods, ultrasound has received particular attention because of its noninvasive nature, deep tissue penetration, and ability to locally activate nanocarriers. This review highlights the recent advances in ultrasound-triggered gas-generating delivery systems, including their design principles, gas-generating mechanisms, and representative nanoplatforms. The mechanistic insights into ultrasound-induced cavitation, thermal effects, and sonodynamic activation are discussed in the context of controlled gas release and drug delivery. Moreover, the therapeutic applications of these systems in solid tumors and metastatic lesions are summarized, and combination strategies integrating

☆ This article is part of a Special issue entitled: 'Gas Delivery' published in Advanced Drug Delivery Reviews.

* Corresponding authors.
E-mail addresses: hyuncheol@sogang.ac.kr (H. Kim), kimkm@ewha.ac.kr (K. Kim).

[1] These authors made equal contribution to this work.

[2] Given their role as Theme Editor, Hyuncheol Kim had no involvement in the peer review of this article and has no access to information regarding its peer-review. Full responsibility for the editorial process for this article was delegated to another journal editor.

https://doi.org/10.1016/j.addr.2025.115747
Received 13 August 2025; Received in revised form 1 November 2025; Accepted 3 December 2025
Available online 4 December 2025
0169-409X/© 2025 Elsevier B.V. All rights are reserved, including those for text and data mining, AI training, and similar technologies.

ultrasound-triggered gas release with chemotherapy, immunotherapy, or phototherapy are outlined. Finally, the current challenges and future perspectives for clinical translation are addressed, focusing on improving safety, scalability, and patient-specific tailoring. Ultrasound-responsive gas-generating delivery systems represent a promising approach for spatiotemporally controlled cancer therapy.

1. Introduction

One of the major factors that decrease the effectiveness of radiation therapy and other anticancer treatments is the hypoxic environment of deep-seated tumors [1,2]. To address this, the precise spatiotemporal control of therapeutic gas delivery has emerged as a critical challenge and promising strategy in the field of oncology [3–5]. Therapeutic gases, including oxygen (O_2), carbon dioxide (CO_2), and nitric oxide (NO), not only resolve hypoxic environments but also provide unique biological effects that can modulate the tumor microenvironment to enhance treatment outcomes (Table 1). However, these agents' clinical translation is severely limited by a fundamental obstacle inherent to their physical state: the lack of controlled delivery. Compared with conventional solid or liquid drugs, gases are inherently highly diffusive and difficult to contain locally [6,7]. Once released, the rapid expansion of gases can lead to significant off-target damage to healthy tissues. Furthermore, this same diffusive property makes it increasingly difficult to maintain a therapeutically meaningful concentration at the tumor site, often rendering treatments ineffective. Consequently, sophisticated delivery systems that can release gaseous payloads "on demand" at the intended location need to be developed. Among various external triggers, gas delivery systems with ultrasound triggered release have emerged as a particularly promising candidate to achieve this requisite on-demand control [8].

Table 1
Summary of therapeutic gases and their core anticancer mechanisms.

Therapeutic gas	Anticancer mechanisms	Key references
Nitric oxide (NO)	NO induces significant oxidative stress at high concentrations (>500 nM). This leads to DNA damage, lipid peroxidation, activation of proapoptotic proteins, and inhibition of cellular respiration, thereby causing mitochondrial dysfunction and cancer cell apoptosis.	[29–31]
Carbon monoxide (CO)	CO induces an "anti-Warburg effect" by targeting mitochondria. It forces cancer cells to increase oxygen consumption and oxidative phosphorylation, which lead to a surge in reactive oxygen species (ROS), metabolic exhaustion, and collapse of mitochondrial function, thereby triggering apoptosis and mitotic catastrophe.	[32,33]
Hydrogen sulfide (H_2S)	Therapeutic concentrations of exogenous H_2S disrupt the mitochondrial electron transport chain, inhibiting the production of adenosine triphosphate and causing bioenergetic stress. It induces ROS-mediated apoptosis through pathways involving the activation of extracellular signal-regulated kinase and mitogen-activated protein kinase. H_2S can also arrest the cell cycle and synergize with other therapies.	[34,35]
Hydrogen (H_2)	H_2 acts as a selective antioxidant that specifically neutralizes the most cytotoxic ROS, thereby reducing oxidative-stress-induced cellular damage. It can mitigate the side effects of chemotherapy and radiotherapy without compromising their antitumor efficacy.	[36]
Oxygen (O_2)	O_2 works by increasing the partial pressure of O_2 to overcome tumor hypoxia. This re-oxygenation makes hypoxic, therapy-resistant cancer cells more susceptible to the cytotoxic effects of radiation and certain chemotherapies by increasing the local production of tumor-damaging free radicals.	[37–39]
Carbon dioxide (CO_2)	The transcutaneous or localized delivery of CO_2 can induce the Bohr effect, where an increase in CO_2 concentration and a decrease in pH cause hemoglobin to release more O_2, thereby alleviating tumor hypoxia. CO_2 can also directly induce apoptosis through mitochondrial pathways and modulate the tumor microenvironment.	[40–43]
Sulfur dioxide (SO_2)	SO_2 induces cancer cell apoptosis by increasing intracellular ROS levels, causing nuclear DNA damage, activating the executioner caspase-3, and downregulating the expression of the anti-apoptotic protein Bcl-2.	[44,45]

The use of nanomaterial-based delivery systems has gained considerable attention as an effective alternative. These systems can encapsulate chemically reactive or volatile gas-generating compounds and directly entrap gas molecules, offering a means to stabilize these agents within the biological environment and prevent unintended diffusion or activation before reaching the tumor site [9–11]. Moreover, surface modifications, including the conjugation of polyethylene glycol or attachment of tumor-targeting ligands, enhance selective accumulation within tumor tissues through passive and active targeting mechanisms [12–14]. Consequently, gas release can be confined to tumor regions, thereby minimizing potential damage to healthy tissues. These systems can also be engineered to respond to specific features of the tumor microenvironment, including low pH, increased reactive O_2 species, and high glutathione concentrations, thereby enabling precise control over gas release [15–17]. Furthermore, their modular architecture supports the co-delivery of therapeutic agents, including anticancer drugs and immune-stimulating molecules, facilitating synergistic treatment outcomes [18]. Collectively, these attributes highlight the potential of nanomaterial-based platforms as versatile and effective tools for achieving controlled gas delivery in cancer therapy.

Ultrasound is a suitable noninvasive trigger system because of its well-established clinical safety profile, remarkable controllability, and multifaceted therapeutic effects [19,20]. Furthermore, ultrasonic waves facilitate precise spatiotemporal regulation, thereby enabling targeted activation at a designated moment in time [21,22]. Ultrasound's safety profile is well documented, and its uses in clinical imaging and therapeutic interventions are well established [23,24]. Furthermore, ultrasound parameters, including the frequency, intensity, and duty cycle, can be meticulously regulated to customize the interaction of ultrasound with gas-carrying particles [25]. For example, low-intensity, low-frequency ultrasound effectively releases encapsulated gas payloads by inducing acoustic cavitation, defined as the vibration and subsequent collapse of gas bubbles [26]. Furthermore, pulsed ultrasound, which is characterized by low duty cycles, can be used to optimize mechanical effects while minimizing the occurrence of unwanted tissue heating [27]. Aside from its role in inducing gas release, ultrasound also confers additional therapeutic benefits. Microbubble or nanocarrier cavitation can temporarily disrupt cell membranes and open up tight junctions in blood vessels, thereby improving drug absorption and O_2 perfusion in deep-seated tumors through sonoporation [28]. The localized nature of ultrasound's effect enables gas-loaded carriers to circulate in an inactive state until they are activated at the tumor site. These external controls offer a high degree of specificity, which enables the precise targeting of therapeutic gases to the tumor site and enhances treatment outcomes, thereby reducing the necessity for invasive procedures.

Ultrasound-triggered gas delivery systems (UTGDS) not only address major clinical challenges (e.g., tumor hypoxia and limited therapeutic precision) but also provide a noninvasive means to achieve spatiotemporally controlled gas release. Therefore, the integration of gas therapy, nanomaterials, and ultrasound into a unified platform has become increasingly essential. UTGDS offer a promising strategy to enhance therapeutic efficacy, minimize systemic toxicity, and bridge the current translational gap in gas-based cancer therapy by combining the biological potency of therapeutic gases with the targeting versatility of nanomaterials and external controllability of ultrasound. Therefore, this review specifically focuses on carrier systems that form the core of UTGDS for cancer therapy (Fig. 1). The initial section delineates ultrasound's physical mechanisms in targeted delivery, including acoustic cavitation and its associated bioeffects. Meanwhile, the subsequent section encompasses the diverse material platforms that are used in UTGDS, including lipid-based particles, polymeric particles, and various organic–inorganic structures, along with their therapeutic applications. With the recent advances in materials science leading to a surge of novel and complex carrier designs, a comprehensive review is critically needed to consolidate these developments and elucidate key structure–function relationships. Finally, the key limitations and challenges of UTGDS, which are uniquely complex considering that they exist at the intersection of three distinct regulatory domains (i.e., gas therapeutics, delivery vehicles, and ultrasound devices), are discussed. This integrated perspective frames our analysis of issues, including safety considerations, achieving uniform gas distribution, and maintaining precise control over dosing and release kinetics. This review aims to highlight existing obstacles and provide a forward-looking perspective to help researchers accelerate the design of next-generation UTGDS for successful clinical translation by systematically analyzing the current landscape.

2. Mechanisms of ultrasound-mediated delivery

2.1. Ultrasound parameters

Medical ultrasound systems are defined by various physical parameters that determine their behavior, safety, and efficacy in targeted delivery. These parameters encompass frequency, acoustic pressure, mechanical index (MI), duty cycle, exposure time, and other variables (Fig. 2). These parameters can be modified to achieve the desired effects.

2.1.1. Frequency

The ultrasound wave frequency is a fundamental parameter that governs the system's behavior. Ultrasound frequencies ranging from low kilohertz (kHz) to several megahertz (MHz) have been used in drug and gas delivery. Lower frequencies ranging from 20 kHz to 500 kHz can penetrate deeper into tissues and more readily induce cavitation effects, making them effective for enhanced permeability, including sonoporation [46–48]. Higher frequencies, which exceed 1 MHz, can provide enhanced precision in focalization. However, these frequencies necessitate higher pressures to achieve the desired cavitation level. Indeed, several studies employing microbubble-mediated delivery have utilized frequencies in the range of 1 MHz, thereby ensuring the optimal responsiveness of microbubbles with a diameter of 1–3 μm to the acoustic field [49]. For example, a 1-MHz ultrasound field has been shown to effectively drive standard microbubble contrast agents [50]. By contrast, higher frequencies tend to produce only linear oscillations and require higher intensities to achieve comparable effects. In practice, frequency selection is contingent upon the target depth and the gas vehicle's dimensions and resonance. That is to say, lower frequencies are used for deeper targets and stronger cavitation, whereas higher frequencies are utilized for superficial targets or precision guided by imaging [51,52].

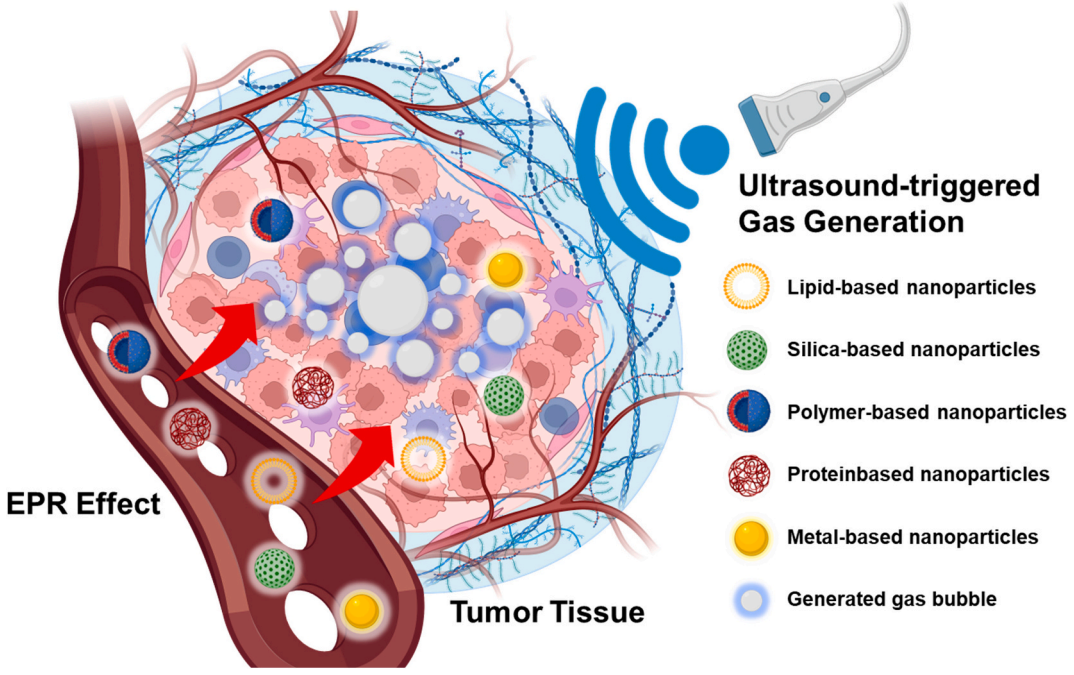


Fig. 1. Schematic of ultrasound-triggered gas-generating nanomedicine for tumor-targeted delivery and therapy. Various gas-generating nanoparticles are systemically administered and accumulate in the tumor tissue via the effect of enhanced permeability and retention (EPR) or active targeting. These nanocarriers undergo structural disruption or phase transition upon localized ultrasound irradiation, resulting in the controlled release of therapeutic agents and in situ generation of gas. The generated gas bubbles not only enhance intratumoral drug penetration through acoustic cavitation and improved vascular permeability, but also serve as contrast agents for ultrasound imaging, thereby enabling real-time theragnostics. This strategy allows for spatiotemporally controlled release of drugs and gases, thereby enhancing the therapeutic efficacy while minimizing off-target toxicity. Created in BioRender. Moon, J. (2025) https://BioRender.com/jc0643r

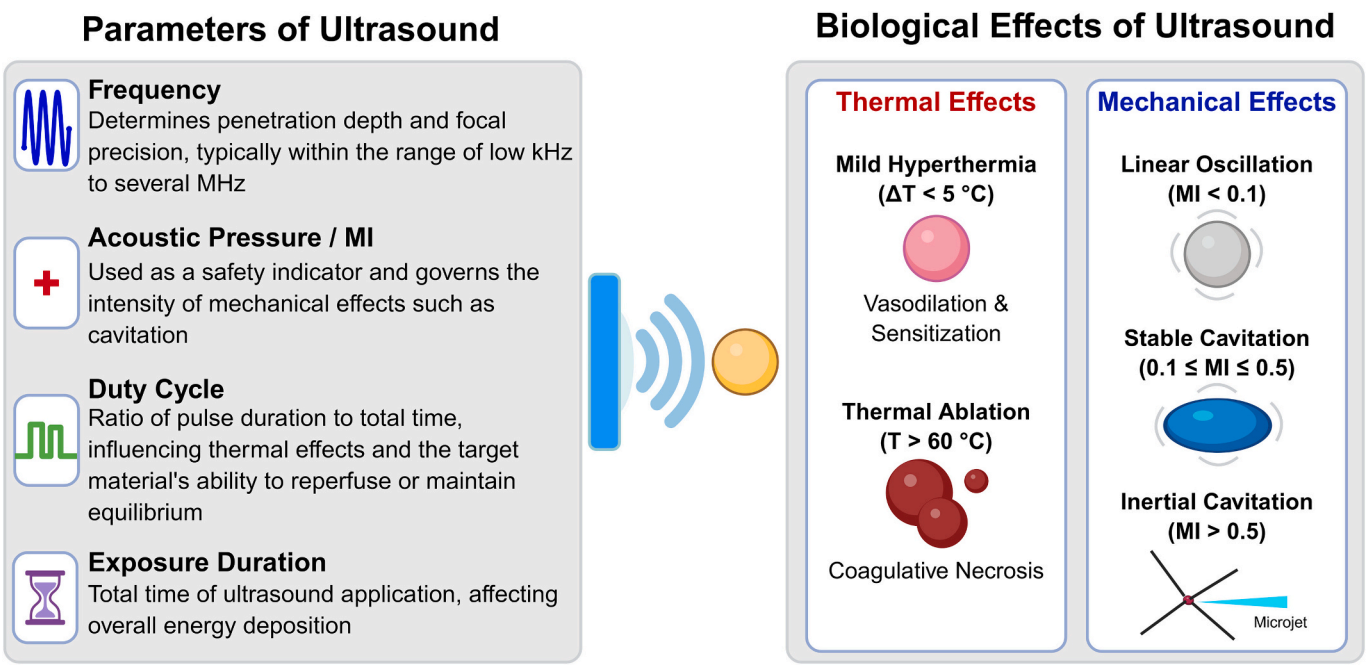


Fig. 2. Schematic of the parameters and biological effects of ultrasound. Medical ultrasound systems are governed by a multitude of parameters, including frequency, acoustic pressure, duty cycle, and exposure duration. By adjusting these parameters, a variety of thermal and mechanical effects can be applied to the target area or target drug. Created in BioRender. Moon, J. (2026) https://BioRender.com/8n8hqg0

2.1.2. Acoustic pressure and MI

The MI, which is defined as pressure divided by the square root of frequency, has been identified as a convenient safety metric [53]. The regulatory guidelines for diagnostic ultrasound establish an MI limit of 1.9 in human imaging. In controlled therapeutic applications, researchers may deliberately use MI values of 0.5–1.5 to trigger drug or gas release, balancing efficacy with safety [49,54]. The ultrasound amplitude exerts a substantial influence on microbubbles' oscillatory behavior, dictating whether they oscillate gently or collapse violently.

A threshold of a few hundred kilopascals (approximately over 0.5 MPa at 1 MHz, corresponding to an MI over 0.5) is typically needed to induce inertial cavitation, which involves the violent collapse of microbubbles [55]. This collapse generates intense and localized physical forces, resulting in shock waves and microjets. These forces result in the formation of pores, measuring hundreds of nanometers in size, in the cell membrane. This substantial disruption facilitates the direct delivery of large therapeutic agents, including nanoparticles and gene complexes, which are difficult to deliver directly into cells using conventional methods. However, this aggressive mechanism has a high risk of causing cell damage and apoptosis.

Microbubbles undergo stable (non-inertial) cavitation at moderate pressures (often in the MI range of 0.1 to 0.5), repeatedly expanding and contracting in a nonlinear yet nondestructive manner [56]. This oscillation generates a fluid flow, which exerts shear stress on the cell membrane. This stress can deform the membrane, leading to the formation of small, reparable pores. Aside from the formation of small pores, the mechanical stress induced by stable cavitation stimulates the cell's natural uptake pathways, including endocytosis. This phenomenon is especially pertinent in the context of the uptake of larger molecules, which cannot traverse narrow pores with ease. The formation of these small pores and endocytosis stimulation imply that stable cavitation is a safer and more controllable method for delivering small molecules while minimizing cell death.

Only minor linear oscillations occur at acoustic pressures corresponding to an MI under 0.1 [57]. In such symmetrical vibrations, the amount of gas that is dissolved into the surrounding liquid when the bubble expands is equal to that of gas escaping when the bubble contracts. Consequently, the bubble size remains constant over time, which is the primary reason why the vibration effect is described as "minor". Considering the absence of alterations in the bubble size and minimal oscillation amplitude, linear oscillations are not conducive to the robust microstreaming phenomenon observed in stable cavitation. Consequently, oscillations of this magnitude are postulated to have minimal influence in altering cell membrane permeability or enhancing drug absorption.

2.1.3. Pulse repetition frequency (PRF) and duty cycle

Ultrasound can be applied in two modes: pulsed or continuous wave. In the drug delivery domain, pulsed ultrasound has emerged as a prevalent method. This technique is distinguished by the PRF (pulses • s^{-1}), which signifies the frequency at which ultrasound is irradiated, and duty cycle (%), which denotes the proportion of time the ultrasound is exposed during a single cycle. Typical duty cycles range from 0.1% up to 50%, or even 100% for true continuous exposure [58–62]. The use of shorter pulses with rest intervals, or a lower duty cycle, is advantageous because of its capacity to diminish heat deposition in tissues and enable microbubbles to reperfuse or equilibrate between bursts. Compared with a higher PRF, a lower PRF (ranging from 1 Hz to 100 Hz) enables a prolonged interval between successive bursts. This extended time interval facilitates the circulation and introduction of new microbubbles into the target area, thereby preventing the agent's complete destruction in a single instance. According to research, decreasing the PRF and increasing the pulse length can enhance the inertial cavitation effect. This combination has been demonstrated to increase the energy per burst and the likelihood of sustained bubble activity [63]. For example, Tu et al. found that longer pulses and lower PRF resulted in enhanced cavitation and drug delivery, presumably because the microbubbles had sufficient time to replenish the ultrasound field and were exposed to a greater number of acoustic cycles per pulse [64]. In practice, researchers frequently use millisecond-scale pulses (e.g., 1–10 ms bursts) repeated at a rate of approximately 1–100 Hz for several minutes during therapy. This pulsed scheme maximizes the mechanical effects while minimizing thermal buildup.

2.1.4. Exposure duration

The total duration of ultrasound exposure can range from a few seconds to several minutes, depending on the acoustic intensity, duty cycle, and type of tissue involved. Prolonging ultrasound exposure, which increases the cumulative acoustic energy, has been shown to enhance the efficacy of drug- or gas-carrier disruption and transient tissue permeabilization. However, this enhancement is not unlimited and is subject to inherent limitations. Beyond that point, the presence of cavitation nuclei becomes depleted, and the tissues approach a saturation state. Consequently, additional energy produces diminishing or even negative returns. In circumstances involving high-intensity or high-duty-cycle settings, the prolonged fixed positioning of the beam can result in hazardous thermal rise and cumulative mechanical damage. Conversely, low-average-power regimens (e.g., duty cycle ≪1%, spatial-peak temporal-average intensity <500 mW • cm^{-2}) may be endured for extended periods without substantial heating. Consequently, in vivo studies for focused blood–brain barrier (BBB) opening have reported exposure durations ranging from less than 1 s to 20 min, with certain tumor and vascular applications citing figures on the order of 1–5 min per target [65–67]. Several groups have adopted multistage schemes. One potential approach involves an initial high-pressure burst, which is intended to induce cavitation or disrupt vasculature. This is followed by a low-duty-cycle, low-pressure pulsed ultrasound, which sustains bubble activity while maintaining low average power. This strategy has been shown to enhance drug deposition, as demonstrated by Xu et al. [68]. Researchers have developed several protocols to address this issue. Some of these protocols involve the intermittent repetition of high-pressure bursts, whereas others involve the maintenance of a single moderate setting for the duration of the session. In the final analysis, the optimal exposure time is determined empirically for each device–tissue–agent combination, balancing delivery efficiency against thermal and mechanical safety limits. Precisely calibrating the frequency, peak pressure, pulse length, PRF, duty cycle, and total exposure is imperative as each parameter demonstrates a range in which benefits plateau or adverse effects manifest once that threshold is surpassed.

2.2. Bioeffects of ultrasound

Ultrasound interacts with biological tissues primarily through thermal and mechanical mechanisms [69]. The bioeffects resulting from these interactions are governed by the previously discussed ultrasound parameters and subject to variation according to the modality employed.

The absorption of ultrasound energy by tissues result in thermal effects, causing an increase in temperature [70–72]. In the context of diagnostic imaging, the low duty cycle and limited intensity of ultrasound energy ensure minimal tissue heating, typically resulting in a temperature increase of less than 1 °C. The thermal index is a metric that guides clinicians in maintaining exposures within safe boundaries [73]. Conversely, the objective of therapeutic ultrasound, including high-intensity focused ultrasound (HIFU), is to generate substantial heat [74]. In HIFU, the application of focused ultrasound beams can rapidly increase temperatures to 60 °C–100 °C, leading to protein denaturation and coagulative necrosis within a confined area. This high-temperature exposure leads to cell death, making HIFU a potent modality for ablating tumors or other pathological tissues. By contrast, low-intensity focused ultrasound (LIFU) functions at a sub-ablative level, inducing a more nuanced thermal effect that frequently results in mild hyperthermia, which leads to a temperature increase of a few degrees Celsius [75]. These effects can enhance perfusion or sensitize cells to therapeutic agents without causing irreversible damage.

Ultrasound's mechanical effects are mediated by acoustic pressure variations that can induce tissue displacement, stress, and cavitation. In diagnostic applications, the mechanical effects of ultrasound are minimal because of the low intensities and short pulse durations employed [76]. Conversely, in therapeutic applications, mechanical interactions are deliberately exploited for specific therapeutic purposes. For example, in HIFU, high acoustic pressures can induce inertial cavitation, wherein the microbubbles formed from dissolved gases within the tissue rapidly expand and collapse [77,78]. This process gives rise to shock waves and microjets, which disrupt tissue structures. By contrast, LIFU prioritizes the attainment of stable cavitation in the presence of microbubbles [79,80]. The presence of microbubbles enables the generation of stable cavitation, where low-intensity focused pulses induce controlled oscillations without violent collapse. Subsequently, these oscillations give rise to microstreaming and shear forces, which transiently permeabilize cell membranes (i.e., sonoporation), thereby enhancing drug or gene uptake. Aside from cavitation, ultrasound also exerts acoustic radiation force, wherein the momentum transfer from the ultrasound beam can cause slight tissue or fluid displacement [81]. This force can be used to manipulate microbubbles, thereby enhancing their interaction with cell membranes or even aiding in the repositioning of therapeutic agents. However, ultrasound's bioeffects are not solely contingent on the ultrasound beam power but are also influenced by the exposure duration and tissue's acoustic properties. For example, higher absorption rates in bone tissues can result in greater temperature elevations compared with those in soft tissues when exposed to identical ultrasound intensities.

Achieving a balance between these effects is imperative in the context of UTGDS. However, there are numerous variables that complicate control. The objective is to generate sufficient mechanical disruption to enable therapeutic delivery, including overcoming the BBB or targeting deep-seated tumors, while avoiding irreversible damage or off-target safety issues. To achieve this objective, ultrasound parameters need to be precisely calibrated, and real-time monitoring and feedback mechanisms need to be implemented. These mechanisms are essential to ensure that biological effects remain within the desired range. In summary, understanding the interactions between thermal and mechanical biological effects is important for designing ultrasound protocols that optimize therapeutic benefits while minimizing collateral damage.

3. Diverse material platforms for UTGDS in Cancer

The use of UTGDS constitutes an emerging strategy within the domain of oncology, which facilitates the regulated transport and subsequent release of various therapeutic gases to tumor sites. The materials used for UTGDS can be broadly categorized into the following groups: lipid-based, silica-based, metal-based, polymer-based, protein-based, and other groups (Table 2). These materials possess promising potential for the precise and targeted delivery of therapeutic gases to specific tumor sites because of their capacity to accurately and safely respond to ultrasound, whether utilized alone or in combination. This section introduces various material platforms that are used in UTGDS. In this section, the emergence of each material group is analyzed to address specific clinical and technical challenges. Moreover, the new limitations encountered in the process and their subsequent evolution are examined to overcome these obstacles. Each platform exhibits distinct strengths and weaknesses with regard to stability, gas loading efficiency, in vivo behavior, and clinical translation potential. This section will provide a systematic comparison and evaluation of these characteristics.

3.1. Lipid-based UTGDS

Lipids are amphiphilic molecules that are characterized by hydrophilic heads and hydrophobic tails. When placed in an aqueous environment, these particles self-assemble to create liposome-like or other micelle-like nanostructures. These nanostructures can encapsulate hydrophilic and hydrophobic medications in their core and membrane, respectively [82]. In the field of UTGDS, significant attention has been directed toward lipid-based carriers because of their distinctive physicochemical properties and biocompatibility [83]. The main types of lipid-based UTGDS for gas transport are microbubbles and echogenic

Table 2
Summary of diverse materials for ultrasound-triggered gas delivery systems.

Type of UTGDS	Advantages	Limitations	Relative Clinical Applicability	Type of Payloads	Payload Loading Methods	Acoustic Conditions	Gas Release Efficiency	Cancer Type	References
Lipid-based	Outstanding biocompatibility and natural self-assembly, protective shell, echogenic	Opposing size requirements for delivery and therapeutic effect. Susceptible to the disruption by blood component, leading to leakage of the encapsulated gas or gas releasing precursor.	Very High [134,135]	O_2 Gas	Infusion	2 MHz, 1000 cycles, MI: 1.4	6 mmHg (in vivo)	Prostate cancer	[89]
				L-arginine	Homogenization emulsification method	1 MHz, 1.5 W/cm^2, 60 s	NO >1 μM (in vitro)	Hepatocellular carcinoma	[136]
				CO Gas	Infusion	1 MHz, 1 W/cm^2, 50% duty cycle, 5 min	74.1 ± 7.8% (in vitro)	Breast cancer	[137]
Silica-based	High loading capacity, good stability, easy modification of shell, tunable pore size.	Slower biodegradation, potential for cytotoxicity, aggregation possibility.	Mid [138–140]	L-arginine	Diffusion	1.0 W, 20% duty cycle, 15 s	4.4 ± 0.4 to 12.5 ± 1.1 μM (in vitro)	Pancreatic cancer	[29]
				SNO(NO donor)	Coavalent bond Conjugation	1 W/cm^2, 10 min	1.22 ± 0.18 to 15.00 ± 0.25 μM (in vitro)	Breast cancer	[94]
				L-menthol	Diffusion	3.5 MHz, 350 W, 2 s	Does not include strategic figures	Cervical adenocarcinoma	[96]
Metal-based	Intrinsic catalytic activity, acoustically responsive., imaging agents	Potential for heavy metal toxicity and long- term bioaccumulation	Low [141,142]	L-arginine	Coavalent bond Conjugation	1.0 MHz, 1.5 W/cm^2, duty cycle 50%, 2 min	About 0.7–2.3 μM NO released (in vitro)	Pancreatic cancer	[99]
				CoOx	in situ growth	1.0 MHz, 0.5 W/cm^2, 1–5 min	CO 2.65 μM (in vitro)	Breast cancer	[143]
				CO	Coordinate bond	0.3 W/cm^2, 15 min	Does not include strategic figures	Breast cancer	[144]
				Poly(CBL-PO)	Coavalent coupling	10 MHz, 0.0676 W/cm^2, MI: 0.235, 30 min	Does not include strategic figures	Squamous cell carcinoma	[147]
Polymer-based	Highly biodegradable Biocompatible versatile.	Risk of premature cargo release.	Mid [145,146]	O_2-saturated PFC	Capillary infusion	1.0 MHz, 1.5 W/cm^2, duty cycle 50%, 2 min	D·O 1.7 times enhanced (in vitro)	Breast cancer	[148]
				L-arginine	Encapsulation	200 kHz, 2 W, 200 s	About 4 times enhanced (in vitro)	Breast cancer	[149]
Protein-based	Low immunogenicity and excellent biocompatibility. Easy modification and targeting.	Sensitive to degradation. Engineered proteins are complex and costly.	Very High [150–152]	PFH	BSA adsorption	1.2 MHz, 4.5 W, duty cycle 2%,	Does not include strategic figures	Cervical adenocarcinoma	[153]
				SNO-HSA	Reversible complexation	1 MHz, 2 W/cm^2, 5 min	NO 6 times enhanced (in vitro)	Breast cancer	[154]
				Bicones	Diffusion	330 kHz, 30 cycles, 0.3 MPa	0–33.7 nM (Agarose phantom)	Glioblastoma	[155]
Others (Hybrid)	Multifunctional by design, synergistic therapeutic	High complexity costly and time consuming.	Relative [156,157]	O_2	Infusion	4.2 MHz, 2.5 MPa	pO2 + 19.7 ± 9.1 mmHg (in vivo)	Breast cancer	[158]
				O_2	Reversible complexation	1.0 W/cm^2, duty cycle 50%, 5 min	About 12 times enhanced (in vitro)	Breast cancer	[159]
				SNO(NO donor)	Coavalent bond conjugation	1 MHz, 1 W/cm^2, duty cycle 20%, 5 min	1.22 ± 0.18 to 15.00 ± 0.25 μM	Breast cancer	[132]

liposomes because of their echogenicity and ultrasound-activated gas release capabilities [84]. During gas delivery, the lipid shells can trap gas molecules or gas-releasing compounds, thereby constraining their release beyond the designated target area and curtailing premature gas dissipation [85]. This protection is imperative for delivering reactive gases, which are generally rapidly absorbed into the bloodstream. Lipid-based UTGDSs are frequently acoustically activated and can release their cargo in a targeted manner in response to external stimuli. When exposed to ultrasonic fields, microbubbles and echogenic liposomes can vibrate or cavitate and can rapidly release the entrapped gases into the surrounding tissue [86,87]. Blum et al. confirmed the acoustic destruction of lipid shell-based microbubbles by ultrasonic pulses [88]. This rupture physically disintegrates micron-sized bubbles, converting them into nanoparticles with an average diameter of approximately 150 nm. The resulting nanoparticles are not mere lipid fragments; rather, they are particles filled with liquid or gas, retaining the original fluorocarbon core. Lipids are the most commonly considered material for UTGDS because of their excellent biocompatibility, targeting capability through ultrasound-activated gas release, and load capacity enabled by their ability to be fabricated in various sizes.

Ho et al. used O_2-MBs to overcome the transient vascular normalization and worsening hypoxia that have been observed in existing antiangiogenic therapies, thereby enhancing vascular maturity, perfusion, and drug delivery [89]. The O_2-MBs used in this study comprised DSPC and DSPE-PEG2000, with a core gas mixture consisting of O_2 and C3F8. The 2-MHz focused ultrasound protocol was applied to the entire tumor to rupture the O_2-MBs and release O_2 while avoiding vascular damage in vivo. The protocol comprised 1000 cycles per pulse at a 2-Hz pulse repetition with an MI of 1.4. The tumor O_2 levels were measured directly during and after acoustic irradiation using an optical fiber pO_2 probe to verify the intended function of the O_2-MBs. A maximum increase in tumor pO_2 of up to 30% was found within 30 min of acoustic irradiation, with an absolute rise reaching approximately 6 mmHg at the 60-min time point. The researchers gradually increased the pressure while imaging vessels in dorsal skinfold chamber models to establish safety and adjust acoustic dose. The results showed that a pressure of 2 MPa induced vasoconstriction without resulting in structural damage, as opposed to a pressure of 3–5 MPa. Furthermore, the results of 24-h hematoxylin and eosin staining did not demonstrate the presence of hemorrhage or necrosis.

Aside from lipid-based microbubble carriers, UTGDS based on nanoplatforms with unique physicochemical and functional properties are also being studied. In the study of Opoku-Damoah et al., a dual-gas lipid nanoplatform was developed to facilitate the ultrasound-activated co-delivery of carbon monoxide (CO) and NO for combined cancer treatment [90]. This system incorporated S-nitrosoglutathione and CO-releasing molecules within a 1,2-dioleoyl-sn-glycero-3-phosphate-based lipid matrix, which was modified with folate for tumor-specific delivery. The lipid membrane provided a protective environment, which maintained the stability of the gas donors during system circulation and enhanced tumor-specific accumulation. Upon exposure to LIFU at 1.25 W/cm^2 for 5 min, the lipid barrier disintegrated, releasing CO and NO gases simultaneously into the tumor microenvironment. The simultaneous gas release induced strong oxidative and nitrosative stress, which overwhelmed cancer cells' antioxidant defenses and promoted cell death. This approach achieved approximately 87% tumor growth inhibition in a colon cancer model compared with monotherapy, demonstrating its potential to improve anticancer efficiency through the controlled, localized release of multiple therapeutic gases.

Nevertheless, the methodology for confirming the successful delivery of lipid-based UTGDS to the target site following its destruction by blood flow and leakage remains a subject of consideration. To address this challenge, Liu et al. developed a magnetic nanoliposome system designed for delivering hydrogen sulfide (H_2S) gas that is capable of dual-mode imaging [91]. This system entrapped anethole dithiolethione (an H_2S precursor) in a lipid bilayer and simultaneously co-entrapped superparamagnetic nanoparticles to enable magnetic field targeting. After these liposomes accumulated in the tumor under an external magnetic field, they were converted into microscopic H_2S gas bubbles in situ, which could be detected by ultrasound imaging. The lipid shell's stability and acoustic reactivity was critical as it protected the H_2S precursor in circulation and contributed to cavitation upon ultrasound exposure. The H_2S-filled lipid bubbles explosively "attacked" and induced mechanical tumor tissue ablation when the tumor site was irradiated with HIFU. At the same time, the released H_2S gas spread to the surrounding cancer cells and triggered biochemical anticancer action as a therapeutic gas carrier. This dual approach combined physical ablation and H_2S-mediated biological therapy to maximize the destruction of cancer cells and significantly improved tumor growth inhibition in vivo. Notably, the entire treatment process was monitored by bimodal magnetic resonance imaging/ultrasound imaging, demonstrating a multimodal gas delivery system for precise cancer theragnostics.

3.2. Silica-based UTGDS

Silica-based nanomaterials are emerging as versatile platforms for delivering therapeutic gases to tumors, particularly in conjunction with ultrasound to trigger or enhance therapy. Silica-based vehicles, which comprise mesoporous silica nanoparticles (MSNs) and hollow MSNs (HMSNs), have been shown to provide a robust means for delivering and releasing gases. MSNs and HMSNs possess a mesoporous framework that combines high loading capacity, biodegradability via disulfide or organosilica linkers, and tunable pore size [29,92–94]. MSNs contain nanoscale pores that can load gas-releasing agents, whereas HMSNs have an interior cavity for a higher payload. These porous structures are well suited for UTGDS as they can store gas-generating molecules and facilitate rapid gas release upon triggering. Ultrasound's mechanical and sonochemical effects, including cavitation and reactive oxygen species (ROS) generation, have been used to facilitate the physical release of cargo from MSNs and HMSNs.

For example, Zhang et al. developed an ultrasound-triggered NO release system that utilizes HMSNs [29]. They loaded and modified the HMSNs with L-arginine and a tumor-targeting aptamer, respectively. Low-intensity ultrasound exposure resulted in the production of ROS, which, in turn, oxidize L-arginine, thereby generating NO. This UTGDS generated NO in a targeted manner, with NO levels exhibiting a substantial increase from 4.4 $\pm$ 0.4 μM to 12.5 $\pm$ 1.1 μM in response to ultrasonic stimulation at 1.0 W and a 20% duty cycle for 15 s at 30-s intervals. In another study, Wang et al. developed a nanoplatform known as MH-SNO@RB [94]. This UTGDS comprised a sonosensitizer, Rose Bengal (RB), and an NO donor (SNO), which were integrated within manganese-doped HMSNs. The MH-SNO@RB was engineered to capitalize on the tumor microenvironment, which is characterized by its acidic and reducing conditions. After 5–10 min of ultrasonic stimulation at 1 MHz, 1.0 W/cm^2, and a 50% duty cycle, the UTGDS enhanced ROS production by releasing RB and SNO. The interaction between these two compounds, which was triggered simultaneously by ultrasound, resulted in the production of highly reactive peroxynitrite (ONOO-). This process amplified the therapeutic impact by inducing a potent cytotoxic effect within the tumor. In addition, this UTGDS demonstrated favorable hemocompatibility and histocompatibility, further substantiating its promising potential as a safe and effective instrument for oncological theragnostic applications.

Nevertheless, the stable structure of HMSNs results in their low ability to induce cavitation in response to ultrasound. To address this issue, Wang et al. reported on perfluorohexane (PFH)-encapsulated mesoporous silica nanocapsules, which are filled with PFH and serve as a landmark example of HMSNs filled with a gas-generating material [95]. These hollow particles measure approximately 150 nm and have a mesoporous silica shell. Moreover, they have demonstrated the capacity for stable circulation within the bloodstream (Fig. 3). The silica shell

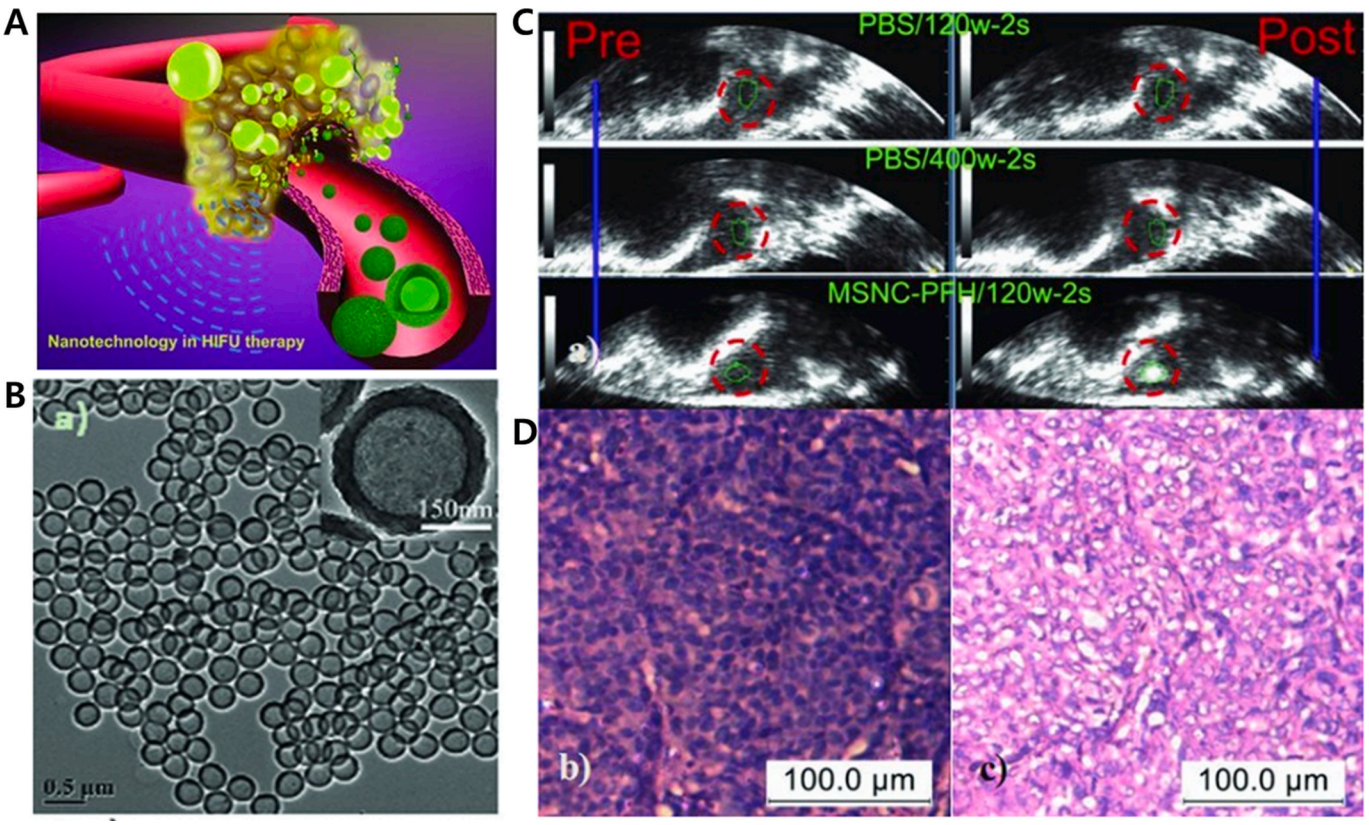


Fig. 3. Ultrasound-responsive perfluorohexane-encapsulated mesoporous silica nanocapsules (MSNC-PFH) for enhanced high-intensity focused ultrasound (HIFU) therapy. (A) Schematic depiction of MSNC-PFH in the blood vessel. (B) Transmission electron microscopy image of MSNC-PFH demonstrating their hollow interior and perfluorohexane loading. (C) Representative ultrasound images taken before and after HIFU exposure, comparing different treatment groups. (D) Histological analysis of tumor sections following treatment shows enhanced tissue ablation in the MSNC-PFH group. Reproduced with permission [95]. Copyright: Wiley-VCH, 2012.

ruptured when 120 W HIFU conditions were applied for 2 s, vaporizing and transforming the PFH core into a gas bubble. This localized enhancement of the effect of HIFU ablation is a notable observation. In the context of tumors, this UTGDS significantly enhanced the tissue-destroying capacity of ultrasound, thereby facilitating "high-efficiency" ablation at reduced HIFU power levels. Moreover, the study introduced the concept of ultrasound-triggered nano-bombs, which undergo a liquid-to-gas phase transition within the silica shell, thereby inducing mechanical damage to cancer cells.

In addition, Zhang et al. developed a novel UTGDS comprising a hollow iron–silica nanoshell filled with L-methanol (LM) that undergoes a "continuous three-phase transition" [96]. They found that the UTGDS can transport drugs or sensitizers with their gaseous precursors. The LM vaporized when exposed to 3.5 MHz and 350 W HIFU for 5 s, breaking the shell and releasing the drug in a controlled burst. This controllable and continuous phase transformation has been demonstrated to enhance the therapeutic effect with each repeated HIFU irradiation, even with a single injection. Facilitated by HIFU guidance, this approach enhances drug delivery with a high degree of precision at the tumor site. In a mouse model, HIFU-triggered drug release from this UTGDS resulted in significantly greater tumor suppression than systemic chemotherapy alone.

3.3. Metal-based UTGDS

The need to produce and control gases more precisely than simply storing them has driven the development of metal-based nanoplatforms (typically using inorganic metal or metal oxide nanoparticles), which have emerged as versatile UTGDS in cancer therapy. These nanomaterials possess several advantageous properties for such applications. First, many inorganic metal nanoparticles have an intrinsic catalytic activity, which can generate therapeutic gases in situ. For example, catalase-mimetic metal oxides can decompose endogenous hydrogen peroxide to O_2, and piezoelectric crystals can split water under acoustic stimulation. Second, these nanoparticles are often acoustically responsive [97,98]. Certain metal-based nanoparticles, including piezoelectric $BaTiO_3$ and ZnO, directly convert the mechanical energy of ultrasound into chemical reactions, enabling on-demand gas release with temporal and spatial control. Furthermore, metal nanoparticles can facilitate ROS generation under ultrasound to synergistically enhance the killing of cancer cells alongside gas therapy. Their surfaces are also readily amenable to functionalization through thiol chemistry and adsorption or coating techniques, which enable the attachment of gas donor molecules, targeting ligands, and additional drugs. Moreover, inorganic nanocarriers tend to be chemically and colloidally stable, which can resist premature gas leakage or degradation during circulation. These features make metal-based UTGDS highly attractive in oncology.

One illustrative example of metal-based UTGDS is piezoelectric barium titanate ($BaTiO_3$) nanoparticles, which generate O_2 gas in response to ultrasound. Wang et al. developed ultrasmall $BaTiO_3$ nanocrystals coated with DSPE-PEG, which act as piezocatalysts to split water molecules in the tumor microenvironment [97]. These UTGDS initiate a redox reaction by generating local charge separation when they are exposed to therapeutic ultrasound at a frequency of 1 MHz, an intensity of 1 W/cm^2, and a duty cycle of 50% for 5 min, resulting in the splitting of water into O_2 gas and ROS. O_2 generation has been demonstrated to alleviate tumor hypoxia, leading to the downregulation of hypoxia-inducible factor 1-alpha and enhancement of the efficacy of ROS-mediated cancer cell ablation. In a breast cancer model, ultrasound-activated $BaTiO_3$ produced sufficient O_2 to significantly

relieve hypoxia and enhance ROS-induced tumor cell apoptosis, thereby inhibiting tumor growth and metastasis. This work demonstrated the stable gas-generating performance of inorganic $BaTiO_3$ and its acoustic responsiveness, highlighting a metal-oxide platform that elevates sonodynamic therapy via on-demand O_2 delivery.

Another powerful strategy involves the use of metal-based UTGDS for NO gas delivery under ultrasound. NO is a gaseous signaling molecule that can induce tumor cell death and modulate the tumor microenvironment. In a previous study, Wang et al. constructed a piezoelectric $BaTiO_3$ nanoplatform co-loaded with an NO donor and a chemotherapeutic drug for ultrasound-triggered NO release for the treatment of pancreatic cancer [99]. The $BaTiO_3$ core generates charge carriers that selectively trigger the decomposition of the attached NO donor under focused ultrasound exposure (1.0 MHz, 1.5 W/cm^2, and 50% duty cycle), resulting in a burst of therapeutic NO gas while simultaneously releasing the co-encapsulated chemotherapeutic drug. The release of NO gas under ultrasound was shown to modulate the extracellular matrix and vasculature of the tumor, transiently increasing its permeability. This effect enhanced the penetration of the chemotherapeutic drug deep into the pancreatic tumor tissue, overcoming the notorious drug delivery barrier in pancreatic tumors. In vivo studies confirmed that the combination of NO gas therapy and chemotherapy had a potent synergistic anticancer effect, significantly inhibiting the growth of the pancreatic tumor. Notably, NO gas also served as an echogenic contrast agent during ultrasound imaging, thereby facilitating image-guided delivery because of the acoustic reflectivity of the released gas bubbles. This example showcases how inorganic piezoelectric UTGDS can achieve on-demand NO gas generation and drug release, leveraging the biological effects of NO (e.g., vasodilation and matrix modulation) to improve therapeutic outcomes.

Notwithstanding the aforementioned advantages, there are concerns regarding the long-term toxicity of metal-based UTGDS. In addition, research on the effects of metal ions after in vivo degradation is limited. Feng et al. used calcium carbonate ($CaCO_3$), a pharmaceutical agent with a well-established clinical profile, to physically generate CO_2 bubbles under ultrasound [100]. This approach induced mechanical tumor damage and improved treatment outcomes. The researchers developed a mesoporous $CaCO_3$ nanoparticle system (MCC-HA) loaded with a sonosensitizer (hematoporphyrin monomethyl ether, HMME) for pH- and ultrasound-responsive gas delivery (Fig. 4). $CaCO_3$ is an inorganic salt that decomposes into calcium ions, water, and CO_2. MCC-HA begins to dissolve in the acidic tumor microenvironment, and ultrasound irradiation at 1 MHz and 1.0 W/cm^2 for 1 min significantly accelerates this process. The UTGDS rapidly decompose when exposed to low pH and ultrasound, simultaneously generating CO_2 gas and releasing the HMME sensitizer. The cavitation of CO_2 bubbles under ultrasound generates strong mechanical shear forces. Furthermore, the oscillation and bursting of bubbles lead to tumor cell necrosis and blood vessel disruption in the tumor tissue, a phenomenon often referred to as the bystander effect. Meanwhile, the released HMME produces ROS in response to ultrasound, resulting in apoptotic cell death through sonodynamic action. In combination, this dual gas/ROS assault achieved remarkable anticancer efficacy in vivo, significantly ablating tumors with minimal off-target toxicity. In addition, the generated CO_2 conferred ultrasound contrast enhancement, allowing the gas-generating nanoparticles (Gas-NPs) to double as an imaging agent for guided therapy. This example highlights the unique advantage of metal-based UTGDS, such as $CaCO_3$. Their inherent chemical reactivity and acoustic sensitivity can be harnessed to produce CO_2 gas on site for inertial cavitation therapy and improved drug/O_2 delivery during

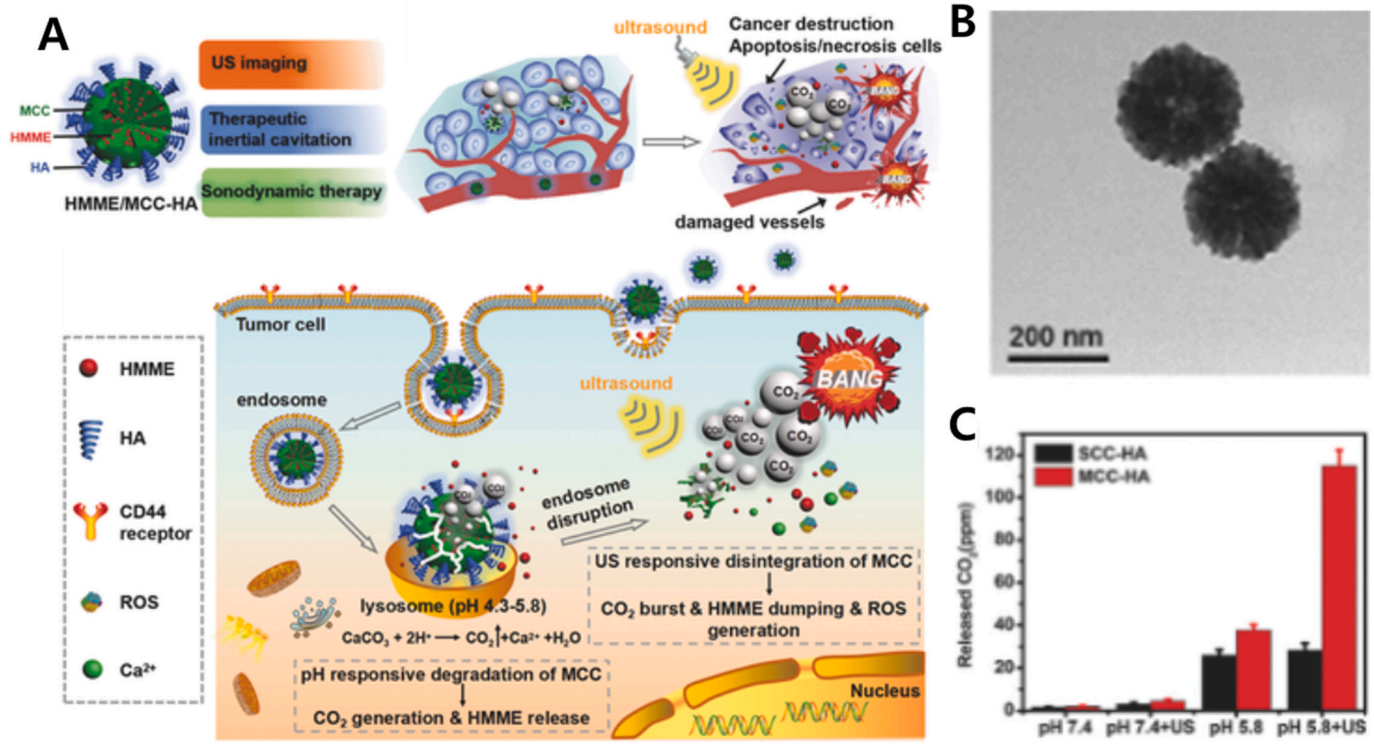


Fig. 4. Schematic and characterization of a pH- and ultrasound-responsive CO_2-generating nanoparticle system for ultrasound imaging and sonodynamic cancer therapy. (A) The mesoporous calcium carbonate ($CaCO_3$) nanoparticle system (MCC-HA) incorporates $CaCO_3$ as a gas precursor, HA for CD44-targeted delivery, and hematoporphyrin monomethyl ether (HMME) as a sonosensitizer. $CaCO_3$ decomposes to release CO_2 and calcium ions (Ca^{2+}) upon uptake by tumor cells and exposure to acidic lysosomal pH, facilitating endosomal escape. Subsequent ultrasound (US) irradiation accelerates MCC collapse, resulting in a rapid burst of CO_2, release of HMME, and production of reactive oxygen species (ROS). This process enhances tumor ablation through combined mechanical cavitation and sonodynamic effects. (B) Transmission electron microscopy image showing the spherical morphology of MCC-HA nanoparticles. (C) The CO_2 release profiles under different pH conditions with and without ultrasound demonstrate synergistic gas generation under acidic and US-triggered environments. Reproduced with permission [100]. Copyright: Wiley, 2017.

ultrasound treatment.

3.4. Polymer-based UTGDS

Polymeric nanoplatforms have attracted considerable interest for ultrasound-triggered gas delivery in cancer therapy. These carriers (e.g., polylactic-*co*-glycolic acid [PLGA] and chitosan) are often biodegradable, have a highly tunable composition and surface functionality, and can stably encapsulate gas donor molecules or gas-generating agents [101]. Their responsiveness to ultrasound stimulation can be controlled by adjusting the polymer structure (e.g., chain length and rigidity) to enable the on-demand release of therapeutic gases at the target site [102]. Polymeric nanocarriers can rapidly release their payload upon exposure to appropriate ultrasound triggers via cavitation-induced mechanical effects or localized heating in the case of HIFU, enabling spatiotemporally controlled gas delivery [82]. This versatility combined with the inherent biocompatibility of many polymers makes them ideal platforms for gas therapy as they can co-deliver conventional therapeutics and gaseous transmitters with ultrasound acting as a remote "on/off" switch.

Min et al. developed a nano-sized chemical gas-generating system based on carbonate copolymers to overcome the limitations of traditional gas-filled ultrasound contrast agents, which often suffer from poor tumor specificity and rapid clearance [103]. In their study, nanoparticles composed of poly(cholesteryl butyrolactone-*co*-propylene oxide) were synthesized to enable in situ CO_2 generation via hydrolysis in the tumor microenvironment (Fig. 5). These Gas-NPs were engineered to remain stable during systemic circulation and to accumulate at tumor sites through the enhanced permeability and retention (EPR) effect. Upon hydrolysis, the carbonate core generated CO_2 nanobubbles, which gradually expanded into echogenic microbubbles, enabling strong and sustained ultrasound signals. Furthermore, anticancer drugs, including docetaxel or doxorubicin (DOX), were co-encapsulated within the Gas-NPs, allowing ultrasound-triggered drug release through the disruption of the CO_2 bubbles. This strategy resulted in enhanced intratumoral drug accumulation and improved therapeutic outcomes in SCC7 tumor-bearing mice, especially when combined with external ultrasound irradiation (40 MHz, 10 min). The UTGDS showed prolonged circulation, strong tumor targeting, and high imaging contrast while minimizing systemic toxicity. This work highlights the potential of chemical gas-generating nanoplatforms for achieving spatiotemporally controlled imaging and therapy in solid tumors.

Yang et al. developed a polymeric UTGDS using PLGA as a carrier for NO delivery [104]. In this design, PLGA nanoparticles encapsulated natural L-arginine as an NO precursor along with iron(II,III) oxide (Fe_3O_4) magnetic nanoparticles, which serve as Fenton catalysts. The PLGA matrix underwent mechanical destruction when exposed to ultrasound at 200 kHz and 2 W for 200 s, resulting in the rapid release of L-arginine and Fe_3O_4 at the tumor site. The freed L-arginine reacted with endogenous H_2O_2 in the tumor microenvironment to generate a burst of NO gas, whereas Fe_3O_4 catalyzed Fenton reactions to produce ROS, which further oxidized L-arginine and amplified the NO output. This ultrasound-triggered cascade achieved potent NO generation in situ, leading to enhanced cancer cell killing, and was validated by significant tumor growth inhibition in a breast cancer model. Notably, the UTGDS showed therapeutic efficacy in vitro and in vivo with minimal systemic toxicity, highlighting the advantage of US-targeted gas release for maximizing antitumor effects while minimizing side effects.

Wen et al. used pollen grains to develop a novel natural polymer microcapsule for the co-delivery of O_2 gas and drugs for synergistic therapy [105]. The hollow sporopollenin exine of sunflower pollen was loaded with an O_2-enriched perfluorocarbon (PFC) liquid and externally adsorbed with DOX (an anticancer drug that can also act as a sonosensitizer), denoted as PO/D-PGs. Exposure to low-intensity ultrasound (1.0 MHz, 1.5 W/cm^2, and 50% duty cycle) for 2 min resulted in acoustic droplet vaporization of the PFC within the pollen, thereby releasing a pulse of O_2 gas directly into the tumor tissue. Concurrently, the ultrasound "excited" DOX, leading to ROS production. This dual action led to a substantial increase in local O_2 levels and ROS generation in tumor cells upon ultrasound stimulation, thereby overcoming hypoxia and enhancing the cytotoxic effect of DOX. In a mouse model of triple-negative breast cancer, ultrasound-activated PO/D-pollen particles effectively inhibited tumor growth compared with chemotherapy or O_2 alone. The combination of O_2 gas delivery and sonodynamic therapy resulted in a synergistic effect, leading to significant tumor cell killing and apoptosis. Of particular significance was the finding that natural

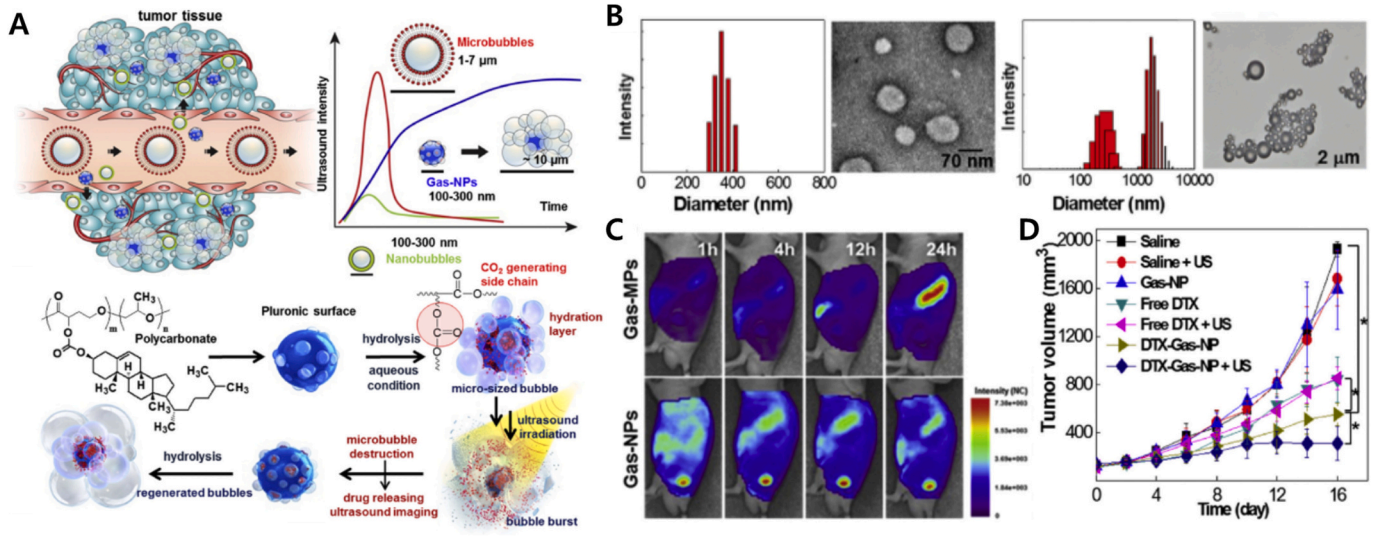


Fig. 5. Schematic and therapeutic evaluation of CO_2-generating nanobubble systems for ultrasound-triggered cancer therapy. (A) Design and mechanism of gas-generating polycarbonate-based nanobubbles, which remain stable under aqueous conditions and undergo hydrolysis to produce CO_2 upon ultrasound exposure. The resulting bubble burst facilitates drug release and ultrasound imaging. (B) Size distribution and transmission electron microscopy/optical microscopy images of gas-generating nanobubbles and microbubbles. (C) In vivo ultrasound imaging of gas-generating microparticles (Gas-MPs) and gas-generating nanoparticles (Gas-NPs) at various time points after intravenous injection, demonstrating distinct retention and signal patterns. (D) Antitumor efficacy of different formulations in a tumor-bearing mouse model, showing superior tumor growth inhibition in the DTX-Gas-NP + US group. Reproduced with permission [103]. Copyright: Journal of Controlled Release, 2016.

pollen-based carriers were biocompatible and biodegradable, demonstrating the potential of bio-derived polymers for gas delivery applications. This study demonstrated the potential of integrating O_2 gas therapy with ultrasound-triggered release, offering a valuable strategy to counteract tumor hypoxia and enhance the efficacy of adjunct treatments.

3.5. Protein-based UTGDS

Protein-based nanoplatforms, including natural proteins (e.g., human serum albumin (HSA), ferritin, and gelatin) and engineered protein assemblies, offer highly biocompatible and versatile vehicles for ultrasound-triggered gas delivery in cancer therapy. These biomolecular carriers are inherently nontoxic and can often evade immunogenicity, especially if they are human-derived; meanwhile, their functional groups and well-defined structures enable easy surface modification or ligand conjugation for targeting [106,107]. HSA is abundant in the blood and tends to accumulate in tumors via the EPR effect, acting as a natural carrier for various endogenous and exogenous ligands [108]. Ferritin nanocages can bind transferrin receptors on cancer cells and can be loaded with therapeutic payloads without eliciting immune responses [109,110]. Gelatin (a denatured collagen) is biodegradable and rich in modifiable functional groups, enabling the fabrication of stimuli-responsive, cross-linkable drug/gas delivery nanoparticles [111–113].

Chang et al. developed PFH-loaded nanodroplets stabilized by a denatured bovine serum albumin (BSA) shell and loaded with IR780 (a hydrophobic sonosensitizer) [114]. These albumin nanodroplets underwent acoustic droplet vaporization into microbubbles followed by inertial cavitation under 10 s of short-pulsed focused ultrasound exposure (1.2 MHz, 4.5 W, and 2% duty cycle) (Fig. 6). The ultrasound trigger released the encapsulated PFH gas as vapor and greatly amplified the sonodynamic effect of IR780. In HeLa cancer cell tests, the PFH@BSA-IR780 nanodroplets produced a surge of ROS and induced rapid cell death upon ultrasound irradiation, achieving a significant drop in viability within 10 s of exposure. The cavitation-induced mechanical damage and ROS generation contributed to cancer cell killing, illustrating how a protein-based nanocarrier can deliver a PFH gas phase on demand to enhance therapeutic outcomes. This albumin/PFH platform demonstrated the feasibility of ultrasound-triggered gas release to boost sonodynamic therapy, leveraging the biocompatibility and strong binding ability of albumin to hydrophobic payloads.

Xu et al. developed an S-nitrosated albumin nanocarrier (SNO-HSA-PTX) that leverages the ability of HSA to form stable S-nitrosothiol bonds as a means of NO storage [115]. In this UTGDS, multiple NO molecules were attached to cysteine-34 of albumin forming S-nitroso-HSA along with the chemotherapeutic drug paclitaxel (PTX), thereby creating a combined gas/drug delivery particle. The SNO-HSA-PTX nanoparticles demonstrated stability within the circulatory system. However, the acoustic energy initiated the release of NO from the S-nitrosothiol groups upon exposure to ultrasound at a frequency of 1 MHz and an intensity of 2 W/cm^2 for during 5 min, as configured within the experimental status. The burst of NO under ultrasound had a profound effect on the tumor microenvironment. NO inhibited tumor-associated platelet activity and "opened" the tumor's vascular barrier, leading to enhanced perfusion and greater accumulation of nanoparticles and T-lymphocytes in the tumor tissue. In murine tumor models, ultrasound-activated SNO-HSA-PTX therapy resulted in a marked increase in intratumoral drug delivery and immune T cell infiltration. It also alleviated tumor hypoxia by facilitating oxygenated blood penetration and significantly inhibited tumor growth compared with controls. This protein-based NO delivery platform demonstrates how ultrasound can remotely trigger a bioreactive release of NO gas from a molecularly engineered albumin carrier, achieving synergistic effects, including enhanced chemotherapy and immunotherapy, through the gas-mediated modulation of tumor vasculature and biology.

However, developing protein nanostructures that can stably encapsulate gases remains a challenging endeavor. Historically, the primary focus of protein-based carriers is the delivery of small-molecule drugs rather than gases. To address this issue, the development of engineered protein structures has emerged as a pivotal research domain. The use of biogenic gas vesicles (GVs) presents a viable solution as they function as stable, air-filled spaces and can be genetically or chemically tailored to ensure stability, targeting, and reactivity [116–128]. Ling et al. introduced GV "bicones" (genetically engineered protein nanostructures derived from microbial GVs) as an innovative ultrasound-responsive gas delivery agent [129]. GVs are essentially hollow protein shells with a

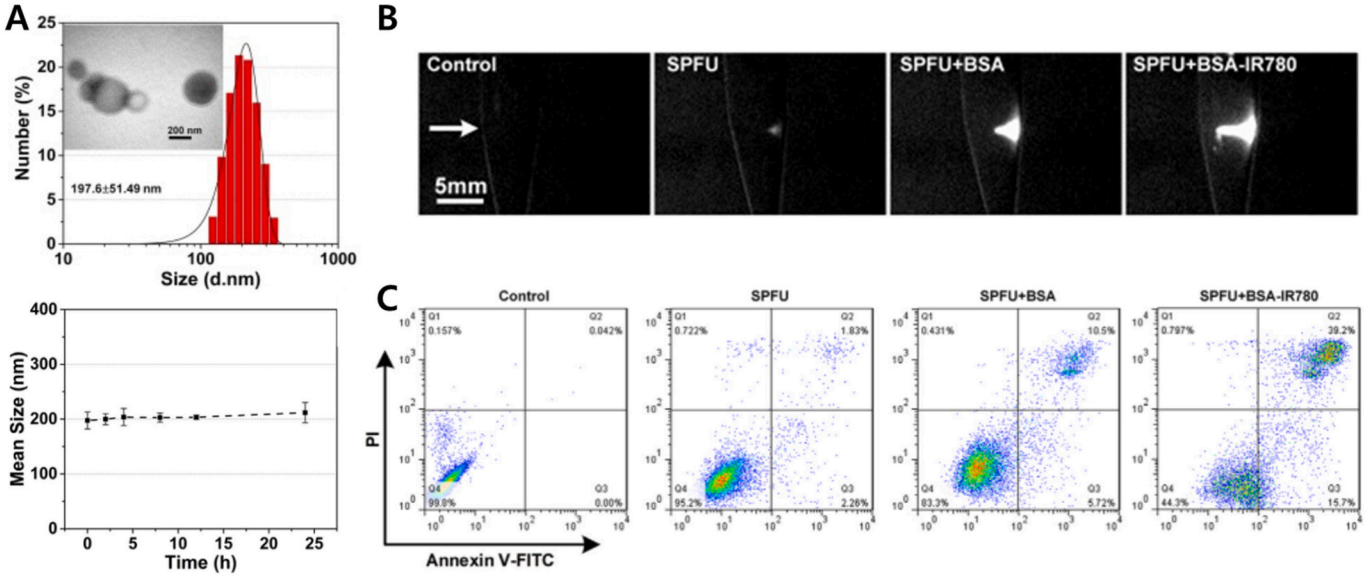


Fig. 6. Characterization and therapeutic performance of SPFU-BSA-IR780 nanoparticles as a sonodynamic gas-generating platform. (A) Dynamic light scattering and transmission electron microscopy analyses demonstrated that the nanoparticles exhibit uniform spherical morphology and good colloidal stability over time. (B) In vivo ultrasound imaging showing enhanced acoustic signals following SPFU-BSA-IR780 administration, indicating ultrasound-triggered gas activation. (C) Flow cytometry analysis demonstrating elevated levels of apoptotic and necrotic cells, supporting the enhanced therapeutic effect mediated by combined sonodynamic and gas-releasing mechanisms. Reproduced with permission [114]. Copyright: Elsevier, 2019.

size of 30–80 nm that can entrap air within their interior. In this work, sub-80-nm bicone-shaped GVs were designed to be systemically injectable and to passively accumulate in tumors via leaky vasculature. These protein-based UTGDSs are inherently echogenic. More importantly, they underwent controlled collapse under HIFU at 330 kHz, 30 cycles, and 0.3 MPa, effectively releasing their internal gas and generating localized mechanical forces. The ultrasound-triggered implosion of GVs produced potent mechanical cavitation effects, which could damage nearby tumor cells or vasculature. In experiments, this UTGDS could be clearly visualized with ultrasound and delivered mechanical perturbations sufficient to cause tumor cell disruption upon activation. These GVs were easily functionalized for molecular targeting and could carry additional payloads on their surface because of their fully proteinaceous, genetically tunable shell. This example highlights the unique potential of engineered protein assemblies, which act as nanoscale gas delivery agents that respond to ultrasound by violently releasing and converting their gas content into therapeutic mechanical energy. These protein-based UTGDS marry the biocompatibility and specificity of biomolecules with the powerful physics of cavitation, offering a novel avenue for noninvasive tumor ablation and drug delivery enhancement.

3.6. Others

In addition to the well-studied lipid-, silica-, metal-, polymer-, and protein-based platforms, researchers have explored various alternative and hybrid UTGDS for cancer therapy, including surfactant-stabilized emulsions/microbubbles and inorganic–organic hybrid nanoparticles [130–132]. These systems offer structurally unique frameworks, such as porous crystalline networks that can be loaded with therapeutic gases and drugs. Moreover, they often exhibit inherent ultrasound responsiveness. For example, liquid PFC cores can undergo acoustic droplet vaporization into gas bubbles, and trapped gases can be liberated via cavitation under ultrasound stimulation. These platforms' modular assembly enables multifunctionality, combining gas delivery with chemotherapy or sonodynamic therapy and even diagnostic imaging. Notably, their nanoscale or bio-derived structures can overcome some limitations of conventional microbubbles, including improved stability, deeper tissue penetration, and prolonged cavitation activity [133].

Eisenbrey et al. developed injectable microbubbles with a surfactant-based shell (termed SE61 O_2) carrying O_2 gas for tumor radiosensitization [130]. These UTGDS cavitate and burst upon ultrasound insonation with 4-MHz pulses at 3.6 MPa, locally releasing O_2 into hypoxic tumor tissue. In breast-tumor-bearing mice, ultrasound-triggered O_2 release increased intratumoral pO_2 within 20 mmHg and was independent of blood hemoglobin transport, enabling oxygenation even in avascular tumor regions. Importantly, the ultrasound activation of O_2 microbubbles immediately before radiotherapy nearly tripled the tumor's sensitivity to radiation, yielding approximately 30 extra days of tumor growth control and significantly prolonged survival compared with controls. Thus, this surfactant-stabilized platform provided an enhanced ultrasound contrast agent and a therapeutic O_2 delivery vehicle, dramatically improving radiotherapy outcomes in vivo.

Zhang et al. developed a metal–organic framework (MOF)-based nanoplatform loaded with an ultrasound-sensitive azo compound to achieve dual gas and ROS release [131]. In this design, a porous zirconium MOF bearing porphyrin ligands was loaded with 2,2′-azobis[2-(2-imidazolin-2-yl)propane] (AIPH, an alkyl azo initiator). Upon ultrasound exposure at 1 MHz and 1.0 W/cm^2 for 1 min, the porphyrin units of the MOF acted as sonosensitizers to produce singlet O_2, whereas the encapsulated AIPH thermally decomposed aided by acoustic energy to generate cytotoxic alkyl radicals and release of nitrogen (N_2) gas. The liberated N_2 gas formed bubbling nuclei that decreased the cavitation threshold and intensified acoustic cavitation, thereby improving nanoparticle penetration in the tumor and amplifying the sonodynamic effect. This MOF–AIPH platform achieved robust anticancer effects even in hypoxic tumor conditions. The combination of ROS and radical generation under ultrasound led to efficient tumor cell killing in vitro and significant tumor growth inhibition in breast-cancer-bearing mice. The study demonstrated a truly hybrid mechanism (N_2 gas generation plus ROS production), translating to enhanced in vivo sonodynamic therapy efficacy in a difficult hypoxic tumor model. Such inorganic–organic hybrids illustrate the modularity of design and powerful therapeutic synergy that ultrasound activation can unlock.

Wu et al. developed lipid–silica hybrid "cerasome" UTGDS that sequentially release ROS and NO when exposed to ultrasound [132]. These structurally resilient cerasomes were self-assembled from siloxane-linked lipids. Their bilayers were incorporated with porphyrin sonosensitizers, their surfaces were coated with S-nitrosothiol groups, and their aqueous cores were encased with DOX. The porphyrins produced a burst of ROS when exposed to ultrasound at 1 MHz, 1.5 W/cm^2, and 20% duty cycle for 5 min, which broke the S–NO bonds on the nanoparticles' surface, resulting in the release of NO gas while simultaneously breaking down the cerosomes to free DOX. This meticulously arranged sequence forms a powerful blend. ROS directly harm cancer cells and serve as biochemical prompts for the release of NO and drugs when needed. The elevated NO levels widen blood vessels and adjust the tumor stroma, allowing improved DOX penetration into hypoxic tumor areas. In combination, localized ROS, NO, and chemotherapy act synergistically to surpass drug resistance and induce greater tumor cell death in vivo compared with any single treatment while reducing systemic side effects. These nanoplatforms featuring multiple triggers and agents emphasize the benefits of hybrid designs. The reason is that single-component systems are unable to offer a stable drug carrier, ultrasound sensitizer, or gas release mechanism simultaneously, nor can they synchronize their release in an ultrasound-controllable sequence.

4. Limitations and future perspectives

Despite the substantial preclinical progress, the clinical translation of UTGDS is an arduous endeavor, characterized by challenges that transcend the confines of biological or engineering obstacles. The intricacies of UTGDS stem from its multifaceted nature as a sophisticated drug–device combination product, situated at the intersection of three distinct regulatory domains: (1) the "drug" (gas therapeutics), (2) the "vehicle" (nanocarrier), and (3) the "trigger" (ultrasound device). Achieving effective clinical translation necessitates a systematic, hierarchical approach, wherein fundamental challenges are addressed to facilitate progression to subsequent stages. This section will critically analyze these translational hurdles at each stage of technological maturation (from foundational science to clinical integration) and provide a forward-looking perspective on the innovative strategies being developed to navigate them (Fig. 7).

4.1. Foundational science

The fundamental limitation is the inherent trade-off in UTGDS design between therapeutic efficacy and biological safety. On the one hand, materials must demonstrate sufficient robustness to ensure in vivo stability and adequate gas loading capacity. On the other hand, they must be biocompatible and capable of degrading into nontoxic byproducts. This phenomenon's intricacies are further compounded by the nature of gasotransmitters, including NO and H_2S. These gasotransmitters can exhibit therapeutic properties at high concentrations but paradoxically promote tumor growth at subtherapeutic levels, highlighting the need for precise dose control [160,161]. Furthermore, several stable inorganic platforms (e.g., silica and certain metals) continue to elicit concerns with regard to their non-biodegradability and possible long-term toxicity because of tissue accumulation.

The future outlook for surmounting these foundational challenges lies in the implementation of "design for safe degradation" and enhanced stability. One emerging solution is using phase-change nanodroplets. These nanodroplets remain in a stable liquid state

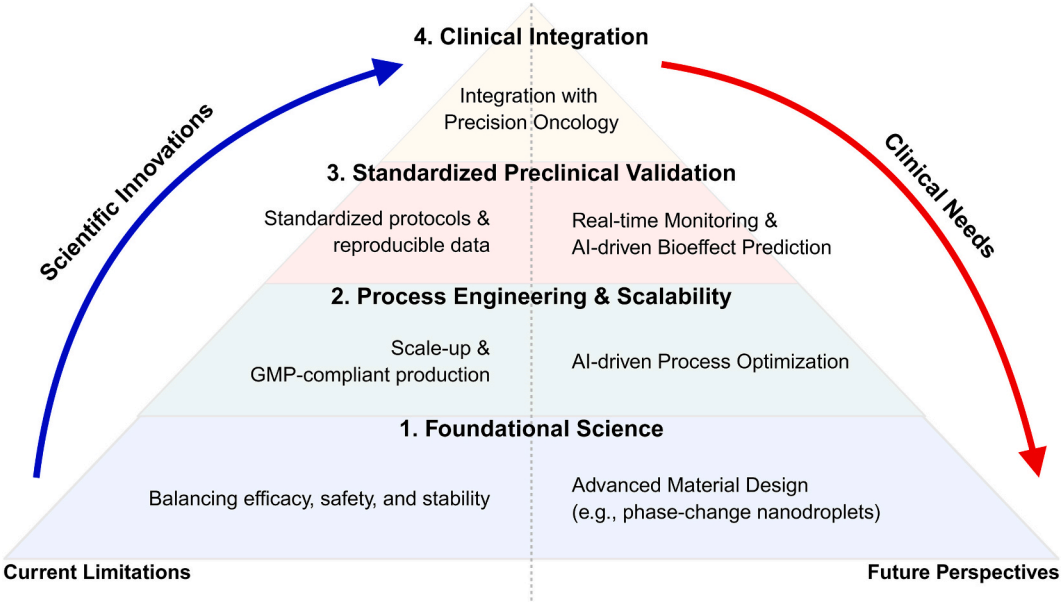


Fig. 7. Schematic of current limitations and future perspectives. Created in BioRender. Moon, J. (2026) https://BioRender.com/8n8hqg0

during circulation and only convert to gas microbubbles when triggered by focused ultrasound, thereby overcoming vascular confinement and improving tumor penetration [162,163]. This strategy enabled in situ gas generation with improved accumulation and retention in tumor tissue, as demonstrated by Zhang et al. using PFC-loaded silica nanocapsules [163]. Another promising avenue is using biogenic GVs, which are genetically encodable, protein-shelled nanostructures with exceptional stability and uniform nanoscale dimensions. Their protein-based composition suggests excellent biodegradability and biocompatibility [129]. Similarly, research into inherently biocompatible inorganic materials, such as $CaCO_3$, which degrades into endogenous ions, offers a pathway to mitigate the long-term toxicity concerns associated with other inorganic platforms [100].

4.2. Process engineering and scalability

Despite the use of optimal materials, there are significant engineering challenges in the transition from laboratory-scale synthesis to large-scale reproducible production that complies with Good Manufacturing Practice (GMP) standards. As mentioned previously, increasing the production volume without altering the characteristics of nano−/microcarriers is a difficult task [164,165]. The inherent variability of existing batch synthesis methods hinders the production of nanoparticles with consistent quality, which is a major failure factor for regulatory approval and clinical use. One approach demonstrated the feasibility of mass production by using a high-shear homogenizer to produce a maximum of 2 L of O_2 microbubbles with a diameter of 2 μm and 90% O_2 by volume in 90 min [166]. Nevertheless, modifications to processes at scaled-up levels still have the capacity to influence parameters, including particle size, gas loading, or stability [167]. Therefore, it is important to ensure batch-to-batch consistency in these key attributes.

The future outlook entails the incorporation of artificial intelligence (AI) into process optimization. The fields of AI, machine learning (ML), and deep learning are evolving into transformative tools that can address these critical challenges. Researchers can predict optimal synthesis parameters to achieve the desired characteristics of nanoparticles by training ML models on extensive datasets. This approach can significantly reduce the time and cost associated with development. For example, Seegobin et al. conducted a study that made use of a comparison between ML-based PLGA production optimization and design of experiments (DOE) [168]. As the analysis progressed with larger datasets, ML not only sustained consistent parameter importance but also furnished more stable and insightful analysis compared with DOE analysis alone.

The recent advances in microfluidic technologies have enabled the production of monodisperse microbubbles with uniform size and shell thickness, thereby enhancing cavitation predictability and in vivo reproducibility. For example, Al-jawadi et al. fabricated lipid-shelled microbubbles with optimized core and shell materials to significantly improve their stability in circulation and acoustic response uniformity [169]. However, microfluidic processes involve multiple nonlinear factors acting simultaneously such as hydrodynamic flow, interfacial tension, and mixing efficiency which makes it difficult to generalize the relationship between process variables and generated particle characteristics using physical models alone [170]. Furthermore, the combination of ML with microfluidics is particularly powerful as it enables microfluidic systems that can produce highly monodisperse nanoparticles with excellent batch-to-batch reproducibility, paving the way for GMP-compliant production. Moore et al. developed a microfluidic ML model that provides formulation parameters for manufacturing specific types of nanoparticles [171]. This model is based on a database comprising three distinct nanoparticle types (i.e., liposomes, lipid nanoparticles, and PLGA nanoparticles). Although these models are not yet applied in the field of UTGDS, they possess the potential to gradually become widespread and evolve into powerful ML-based resources.

4.3. Standardized preclinical validation

A significant challenge in the preclinical validation process is related to the absence of standardized protocols and suboptimal reproducibility of ultrasound bioeffects [172,173]. The optimal ultrasound intensity, frequency, and pulse duration required to reliably trigger gas release in vivo without harming healthy tissues have yet to be determined. Moreover, there is considerable variability in how different carriers respond to ultrasound. The polydisperse populations of UTGDS may not all cavitate or release gas uniformly, leading to inconsistent dosing and poor reproducibility between experiments [174].

The path forward involves a predict-and-control paradigm driven by AI and real-time feedback. Distinct from its role in manufacturing, AI in this stage focuses on therapeutic application. For example, Gatica et al. recently developed a physics-informed ML model to predict the cavitation type (stable vs. inertial), providing a powerful tool to design safer

and more effective protocols [175]. This predictive power should be coupled with real-time monitoring technologies to provide the necessary feedback for control. Recent advancements, including the use of 3D-printed acoustic holograms by Lamothe et al., have led to substantial improvements in the sensitivity and maneuverability of passive cavitation detection systems [176]. This development has enabled the real-time quantification of cavitation doses. Furthermore, Sivasubramanian et al. used photoacoustic imaging to quantify real-time changes in tumor O_2 saturation during sonodynamic therapy, providing a direct measure of therapeutic response [177].

4.4. Clinical integration

Clinical translation is the final and most daunting challenge, which involves navigating stringent regulatory oversight. In the United States, gas-filled microbubbles are classified as drugs. Therefore, nanoparticle-based UTGDS would also be regulated as drug products, requiring compliance with the Food and Drug Administration (FDA) nanomedicine guidelines [178,179]. Moreover, considering that UTGDS integrate a pharmaceutical formulation with an activating ultrasound device, these products are classified as combination products, necessitating the intricate coordination between drug and device review centers [180,181]. Currently, no such system has been approved.

A prospective approach to mitigating these regulatory challenges entails the use of existing human safety data. In recent developments, companies have made collaborative efforts with the FDA to repurpose approved diagnostic microbubbles as therapeutic adjuvants [182]. This strategy is exemplified by ongoing clinical trials that, while not directly testing gas therapy, are de-risking the foundational components of UTGDS. Currently, researchers are performing studies to evaluate the effectiveness of sonoporation with microbubbles in enhancing chemotherapy, as evidenced by ongoing clinical trials for pancreatic cancer and hepatocellular carcinoma (NCT04821284 and NCT03199274, respectively). Furthermore, there are ongoing studies exploring the potential of sonoporation to increase tumor sensitivity to radiation, as demonstrated by clinical trials for breast cancer (NCT04431674) and other cancers [183,184]. These trials fulfill a critical function by validating the safety and feasibility of ultrasound–carrier interaction. In order to substantiate their intricate developmental endeavors, UTGDS are obligated to proffer a distinctive clinical benefit. This value is not merely a standalone therapy, but rather a multifunctional, synergistic platform that can overcome the fundamental limitations of the three pillars of modern cancer care: radiotherapy, chemotherapy, and immunotherapy [184–186]. The strategy of loading O_2 into microbubbles and subsequently bursting them with ultrasound to alleviate tumor hypoxia has already demonstrated promising results in preclinical and early clinical stages by enhancing radiosensitivity [184]. Furthermore, clinical trials employing ultrasound–microbubble-assisted sonophoresis have demonstrated enhanced intratumoral penetration of chemotherapeutic agents without increasing systemic toxicity, suggesting a potential to overcome the limitations of conventional chemotherapy [187]. Furthermore, ongoing clinical trials, including the NCT05317858 trial on non-small cell lung cancer (NSCLC) brain metastasis, are exploring the potential of leveraging this effect in combination with immune checkpoint inhibitors [185]. Moreover, NO- and CO-based gas therapies are being developed as strategies to locally release therapeutic gases in response to ultrasound, thereby inducing cancer cell apoptosis and activating immune cells [188]. Aside from these, light-triggered photothermal nanoplatforms that generate localized heating and NO release, MXene–nitroprusside hydrogels capable of near-infrared-induced sustained NO generation, and piezoelectric nanoparticles that simultaneously produce ROS and NO upon ultrasound activation have been developed [189–191]. Collectively, these advances indicate that UTGDS are evolving beyond a simple physical carrier into a multifunctional therapeutic platform capable of O_2 delivery, immune modulation, and radiosensitization, providing a strong foundation for the development of combination therapies and future clinical translation.

5. Conclusion

UTGDS represent a novel and promising paradigm in cancer therapy as they offer noninvasive, spatiotemporally controlled treatment that can be focused on tumor sites with minimal systemic exposure. According to preclinical studies, combining gas-loaded micro−/nanocarriers with ultrasound can improve the effectiveness of conventional treatments. For example, this approach can enhance chemotherapeutic drug uptake and increase tumor sensitivity to radiation while allowing for lower doses of drugs or radiation and reducing side effects. These encouraging results highlight the unique therapeutic mechanisms that gas delivery under ultrasound can provide (e.g., localized oxygenation, mechanical permeabilization via cavitation, or immune stimulation) distinct from traditional modalities. Looking ahead, the field is poised to address current limitations with innovative strategies that enhance precision, functionality, and therapeutic efficacy. Moreover, efforts toward improved targeting are underway, including functionalizing gas nanocarriers with tumor-specific ligands or antibodies to increase accumulation in cancer tissue. Concurrently, advanced biomaterials are being developed to improve stability and enable precise control over gas release. One of the significant leaps forward involves AI integration to optimize treatment parameters. AI-driven models can analyze complex biological data to fine-tune ultrasound settings (e.g., frequency, intensity, and duration) for specific tumor types and depths, thereby maximizing the release of therapeutic gas while minimizing side effects on healthy tissues. The design of UTGDS themselves is also evolving toward sophisticated, multifunctional platforms. Beyond delivering a single type of gas, next-generation systems are being developed to co-deliver multiple therapeutic agents. These multifunctional nanoplatforms can carry different gas combinations, including NO and CO, or pair a therapeutic gas with chemotherapeutics, sonosensitizers, or immunomodulators. This approach enables synergistic, multipronged attacks on tumors, all triggered by a single, localized ultrasound application. Furthermore, a critical advancement is the development of theragnostic platforms. In this model, gas-releasing nanocarriers also function as contrast agents for ultrasound imaging. This dual capability allows for the real-time visualization of the carrier's accumulation in the tumor, precise guidance of the ultrasound focus, and immediate monitoring of the therapeutic response. These theragnostic systems are crucial for translating this technology into the clinical setting as they offer a higher degree of control and safety. These advanced strategies are already showing promise. For example, in vivo, dual-gas ultrasound-activated systems have demonstrated potent antitumor effects at low doses. In addition, synergistic combination regimens are a compelling future direction. These regimens use ultrasound-triggered gas release to normalize the tumor vasculature or boost immunogenic cell death, thereby enhancing immunotherapy and radiotherapy outcomes. With the early-phase clinical trials of ultrasound-triggered microbubble techniques already underway in oncology (e.g., NCT05317858 for the treatment of NSCLC brain metastases), the groundwork is being laid for translating these increasingly sophisticated technologies into practice. In summary, although challenges remain, UTGDS have opened an exciting frontier in cancer therapy. With continued advances in AI-based optimization, the design of multifunctional and theragnostic carriers, and strategic therapeutic integration, this approach holds considerable potential to improve treatment outcomes and pave the way toward more effective, personalized, and localized cancer interventions in the clinic.

Declaration of competing interest

The authors declare that they have no known competing financial interests or personal relationships that could have appeared to influence the work reported in this paper.

Acknowledgements

This research was supported by the Basic Science Research Program through the National Research Foundation of Korea (NRF), funded by the Ministry of Education, Science, and Technology (RS-2023-00261247), Republic of Korea and by the National Research Foundation of Korea (NRF) grant funded by the Korea government (MSIT) (RS-2022-NR068161) and by the Korea Health Industry Development Institute (KHIDI) grant funded by the Korea government (MOHW) (RS-2023-KH135133).

Data availability

No data was used for the research described in the article.

References

[1] C. Beckers, M. Pruschy, I. Vetrugno, Tumor hypoxia and radiotherapy: A major driver of resistance even for novel radiotherapy modalities, in: Seminars in Cancer Biology, Elsevier, 2024.
[2] L.M. Minassian, et al., Hypoxia-induced resistance to chemotherapy in cancer, in: Hypoxia and Cancer Metastasis, Springer, 2019, pp. 123–139.
[3] C. McEwan, et al., Oxygen carrying microbubbles for enhanced sonodynamic therapy of hypoxic tumours, J. Control. Release 203 (2015) 51–56.
[4] W. Fan, B.C. Yung, X. Chen, Stimuli-responsive NO release for on-demand gas-sensitized synergistic Cancer therapy, Angew. Chem. Int. Ed. Engl. 57 (28) (2018) 8383–8394.
[5] X. Lin, et al., Ultrasound activation of liposomes for enhanced ultrasound imaging and synergistic gas and sonodynamic cancer therapy, Nanoscale Horiz. 4 (3) (2019) 747–756.
[6] W. Gong, C. Xia, Q. He, Therapeutic gas delivery strategies, Wiley Interdiscip. Rev. Nanomed. Nanobiotechnol. 14 (1) (2022) e1744.
[7] Y. Wang, T. Yang, Q. He, Strategies for engineering advanced nanomedicines for gas therapy of cancer, Natl. Sci. Rev. 7 (9) (2020) 1485–1512.
[8] K. Tachibana, S. Tachibana, The use of ultrasound for drug delivery, Echocardiography 18 (4) (2001) 323–328.
[9] W. Gong, C. Xia, Q. He, Therapeutic gas delivery strategies, Wiley Interdiscip. Rev. Nanomed. Nanobiotechnol. 14 (1) (2022) e1744.
[10] J. Lee, et al., Theranostic gas-generating nanoparticles for targeted ultrasound imaging and treatment of neuroblastoma, J. Control. Release 223 (2016) 197–206.
[11] W. Um, et al., Necroptosis-inducible polymeric Nanobubbles for enhanced Cancer Sonoimmunotherapy, Adv. Mater. 32 (16) (2020) e1907953.
[12] M. Kyu Shim, et al., Tumor-activated carrier-free prodrug nanoparticles for targeted cancer immunotherapy: preclinical evidence for safe and effective drug delivery, Adv. Drug Deliv. Rev. 183 (2022) 114177.
[13] N. Abaidullah, K. Muhammad, Y. Waheed, Delving into nanoparticle Systems for Enhanced Drug Delivery Technologies, AAPS PharmSciTech 26 (3) (2025).
[14] P. Chaturvedi, et al., Prodrug-based drug delivery systems: strategic approaches and emerging challenges in targeted therapeutics, Naunyn Schmiedeberg's Arch. Pharmacol. (2025), https://doi.org/10.1007/s00210-025-04570-5.
[15] X. Ling, et al., Glutathione-responsive prodrug nanoparticles for effective drug delivery and Cancer therapy, ACS Nano 13 (1) (2019) 357–370.
[16] Z. Yu, et al., Reactive oxygen species-related nanoparticle toxicity in the biomedical field, Nanoscale Res. Lett. 15 (1) (2020) 115.
[17] W. Gao, J.M. Chan, O.C. Farokhzad, pH-responsive nanoparticles for drug delivery, Mol. Pharm. 7 (6) (2010) 1913–1920.
[18] H. Cho, K. Kim, Multi-functional nanomedicines for combinational cancer immunotherapy that transform cold tumors to hot tumors, Expert Opin. Drug Deliv. 21 (4) (2024) 627–638.
[19] M. Postema, O.H. Gilja, Ultrasound-directed drug delivery, Curr. Pharm. Biotechnol. 8 (6) (2007) 355–361.
[20] S. Mitragotri, Healing sound: the use of ultrasound in drug delivery and other therapeutic applications, Nat. Rev. Drug Discov. 4 (3) (2005) 255–260.
[21] Y. Meng, K. Hynynen, N. Lipsman, Applications of focused ultrasound in the brain: from thermoablation to drug delivery, Nat. Rev. Neurol. 17 (1) (2021) 7–22.
[22] C.P. Phenix, et al., High intensity focused ultrasound technology, its scope and applications in therapy and drug delivery, J. Pharm. Pharm. Sci. 17 (1) (2014) 136–153.
[23] D.L. Miller, et al., Overview of therapeutic ultrasound applications and safety considerations, J. Ultrasound Med. 31 (4) (2012) 623–634.
[24] S.B. Barnett, et al., International recommendations and guidelines for the safe use of diagnostic ultrasound in medicine, Ultrasound Med. Biol. 26 (3) (2000) 355–366.
[25] S.M. Chowdhury, T. Lee, J.K. Willmann, Ultrasound-guided drug delivery in cancer, Ultrasonography 36 (3) (2017) 171.
[26] J. Wu, W.L. Nyborg, Ultrasound, cavitation bubbles and their interaction with cells, Adv. Drug Deliv. Rev. 60 (10) (2008) 1103–1116.
[27] X. Jiang, et al., A review of low-intensity pulsed ultrasound for therapeutic applications, I.E.E.E. Trans. Biomed. Eng. 66 (10) (2018) 2704–2718.
[28] C. Coussios, et al., Role of acoustic cavitation in the delivery and monitoring of cancer treatment by high-intensity focused ultrasound (HIFU), Int. J. Hyperth. 23 (2) (2007) 105–120.
[29] K. Zhang, et al., Ultrasound-triggered nitric oxide release platform based on energy transformation for targeted inhibition of pancreatic tumor, ACS Nano 10 (12) (2016) 10816–10828.
[30] W. Jiang, et al., Nitric oxide induces immunogenic cell death and potentiates cancer immunotherapy, ACS Nano 16 (3) (2022) 3881–3894.
[31] S. Korde Choudhari, et al., Nitric oxide and cancer: a review, World J. Surg. Oncol. 11 (2013) 1–11.
[32] B. Wegiel, et al., Carbon monoxide expedites metabolic exhaustion to inhibit tumor growth, Cancer Res. 73 (23) (2013) 7009–7021.
[33] J. Chai, et al., Carbon monoxide therapy: a promising strategy for cancer, J. Mater. Chem. B 11 (9) (2023) 1849–1865.
[34] X. Cao, et al., A review of hydrogen sulfide synthesis, metabolism, and measurement: is modulation of hydrogen sulfide a novel therapeutic for cancer? Antioxid. Redox Signal. 31 (1) (2019) 1–38.
[35] M.R. Hellmich, C. Szabo, Hydrogen Sulfide and cancer, Chemistry, Biochemistry and Pharmacology of Hydrogen Sulfide (2015) 233–241.
[36] M.N.Z.M. Noor, et al., A systematic review of molecular hydrogen therapy in cancer management, Asian Pacific Journal of Cancer Prevention: APJCP 24 (1) (2023) 37.
[37] C.R. Gordijo, et al., Design of hybrid MnO2-polymer-lipid nanoparticles with tunable oxygen generation rates and tumor accumulation for cancer treatment, Adv. Funct. Mater. 25 (12) (2015) 1858–1872.
[38] T. Lin, et al., O2-generating MnO2 nanoparticles for enhanced photodynamic therapy of bladder cancer by ameliorating hypoxia, Theranostics 8 (4) (2018) 990.
[39] V.S. Hughes, J.M. Wiggins, D.W. Siemann, Tumor oxygenation and cancer therapy—then and now, Br. J. Radiol. 92 (1093) (2018) 20170955.
[40] K. Zhang, et al., CO2 bubbling-based'nanobomb'system for targetedly suppressing panc-1 pancreatic tumor via low intensity ultrasound-activated inertial cavitation, Theranostics 5 (11) (2015) 1291.
[41] M.F. Chung, et al., A liposomal system capable of generating CO2 bubbles to induce transient cavitation, lysosomal rupturing, and cell necrosis, Angew. Chem. Int. Ed. 51 (40) (2012) 10089–10093.
[42] C. Xie, et al., CaCO3-MnSiO x hybrid particles to enable CO2-mediated combinational tumor therapy, Nano Res. 15 (9) (2022) 8281–8290.
[43] J.F.P. Gaspary, et al., Translational insights into the hormetic potential of carbon dioxide: from physiological mechanisms to innovative adjunct therapeutic potential for cancer, Front. Physiol. 15 (2024) 1415037.
[44] S. Li, et al., Near-infrared light-triggered sulfur dioxide gas therapy of cancer, ACS Nano 13 (2) (2019) 2103–2113.
[45] W. Shen, et al., A glutathione-responsive sulfur dioxide polymer prodrug as a nanocarrier for combating drug-resistance in cancer chemotherapy, Biomaterials 178 (2018) 706–719.
[46] S. Mitragotri, D. Blankschtein, R. Langer, Ultrasound-mediated transdermal protein delivery, Science 269 (5225) (1995) 850–853.
[47] S. Mitragotri, D. Blankschtein, R. Langer, Transdermal drug delivery using low-frequency sonophoresis, Pharm. Res. 13 (1996) 411–420.
[48] I. Lentacker, et al., Ultrasound exposure of lipoplex loaded microbubbles facilitates direct cytoplasmic entry of the lipoplexes, Mol. Pharm. 6 (2) (2009) 457–467.
[49] C.-D. Ohl, et al., Sonoporation from jetting cavitation bubbles, Biophys. J. 91 (11) (2006) 4285–4295.
[50] K. Ferrara, R. Pollard, M. Borden, Ultrasound microbubble contrast agents: fundamentals and application to gene and drug delivery, Annu. Rev. Biomed. Eng. 9 (1) (2007) 415–447.
[51] C.-K. Yeh, S.-Y. Su, Effects of acoustic insonation parameters on ultrasound contrast agent destruction, Ultrasound Med. Biol. 34 (8) (2008) 1281–1291.
[52] Y. Jang, et al., Exosome-based photoacoustic imaging guided photodynamic and immunotherapy for the treatment of pancreatic cancer, J. Control. Release 330 (2021) 293–304.
[53] J.G. Abbott, Rationale and derivation of MI and TI—a review, Ultrasound Med. Biol. 25 (3) (1999) 431–441.
[54] Y. Taniyama, et al., Local delivery of plasmid DNA into rat carotid artery using ultrasound, Circulation 105 (10) (2002) 1233–1239.
[55] C.C. Coussios, R.A. Roy, Applications of acoustics and cavitation to noninvasive therapy and drug delivery, Annu. Rev. Fluid Mech. 40 (1) (2008) 395–420.
[56] B.D. Meijering, et al., Ultrasound and microbubble-targeted delivery of macromolecules is regulated by induction of endocytosis and pore formation, Circ. Res. 104 (5) (2009) 679–687.
[57] M. Afadzi, et al., Effect of ultrasound parameters on the release of liposomal calcein, Ultrasound Med. Biol. 38 (3) (2012) 476–486.
[58] S. Mitragotri, et al., Synergistic effect of low-frequency ultrasound and sodium lauryl sulfate on transdermal transport, J. Pharm. Sci. 89 (7) (2000) 892–900.
[59] A. Boucaud, et al., Clinical, histologic, and electron microscopy study of skin exposed to low-frequency ultrasound, The Anatomical Record: An Official Publication of the American Association of Anatomists 264 (1) (2001) 114–119.
[60] S.E. Lee, et al., Penetration pathways induced by low-frequency sonophoresis with physical and chemical enhancers: iron oxide nanoparticles versus lanthanum nitrates, J. Invest. Dermatol. 130 (4) (2010) 1063–1072.
[61] A. Tezel, S. Mitragotri, Interactions of inertial cavitation bubbles with stratum corneum lipid bilayers during low-frequency sonophoresis, Biophys. J. 85 (6) (2003) 3502–3512.

[62] J.E. Seto, et al., Effects of ultrasound and sodium lauryl sulfate on the transdermal delivery of hydrophilic permeants: comparative in vitro studies with full-thickness and split-thickness pig and human skin, J. Control. Release 145 (1) (2010) 26–32.
[63] W.-S. Chen, et al., Inertial cavitation dose and hemolysis produced in vitro with or without Optison®, Ultrasound Med. Biol. 29 (5) (2003) 725–737.
[64] J. Tu, et al., Inertial cavitation dose produced in ex vivo rabbit ear arteries with Optison® by 1-MHz pulsed ultrasound, Ultrasound Med. Biol. 32 (2) (2006) 281–288.
[65] A. Marin, et al., Drug delivery in pluronic micelles: effect of high-frequency ultrasound on drug release from micelles and intracellular uptake, J. Control. Release 84 (1–2) (2002) 39–47.
[66] A. Marin, M. Muniruzzaman, N. Rapoport, Acoustic activation of drug delivery from polymeric micelles: effect of pulsed ultrasound, J. Control. Release 71 (3) (2001) 239–249.
[67] Y.-Z. Zhao, et al., Characterization and anti-tumor activity of chemical conjugation of doxorubicin in polymeric micelles (DOX-P) in vitro, Cancer Lett. 311 (2) (2011) 187–194.
[68] Z. Xu, J.B. Fowlkes, C.A. Cain, A new strategy to enhance cavitational tissue erosion using a high-intensity, initiating sequence, IEEE Trans. Ultrason. Ferroelectr. Freq. Control 53 (8) (2006) 1412–1424.
[69] D. Dalecki, Mechanical bioeffects of ultrasound, Annu. Rev. Biomed. Eng. 6 (1) (2004) 229–248.
[70] A. Shaw, N. Pay, R. Preston, Assessment of the Likely Thermal Index Values for Pulsed Doppler Ultrasonic Equipment-Stages II and III: Experimental Assessment of Scanner/Transducer Combinations, 1998.
[71] J. Jago, et al., A comparison of AIUM/NEMA thermal indices with calculated temperature rises for a simple third-trimester pregnancy tissue model, Ultrasound Med. Biol. 25 (4) (1999) 623–628.
[72] J.S. Abramowicz, et al., Fetal thermal effects of diagnostic ultrasound, J. Ultrasound Med. 27 (4) (2008) 541–559.
[73] T.A. Bigelow, et al., The thermal index: its strengths, weaknesses, and proposed improvements, J. Ultrasound Med. 30 (5) (2011) 714–734.
[74] E. Maloney, J.H. Hwang, Emerging HIFU applications in cancer therapy, Int. J. Hyperth. 31 (3) (2015) 302–309.
[75] J. Liu, et al., Low-intensity focused ultrasound (LIFU)-activated nanodroplets as a theranostic agent for noninvasive cancer molecular imaging and drug delivery, Biomater. Sci. 6 (11) (2018) 2838–2849.
[76] R.S. Meltzer, Food and Drug Administration ultrasound device regulation: the output display standard, the "mechanical index," and ultrasound safety, J. Am. Soc. Echocardiogr. 9 (2) (1996) 216–220.
[77] M. Bailey, et al., Physical mechanisms of the therapeutic effect of ultrasound (a review), Acoust. Phys. 49 (2003) 369–388.
[78] G. Ter Haar, HIFU tissue ablation: concept and devices, Therapeutic ultrasound (2016) 3–20.
[79] J. Liu, et al., Low-intensity focused ultrasound (LIFU)-induced acoustic droplet vaporization in phase-transition perfluoropentane nanodroplets modified by folate for ultrasound molecular imaging, Int. J. Nanomedicine (2017) 911–923.
[80] J. Hou, et al., LIFU-responsive nanomedicine enables acoustic droplet vaporization-induced apoptosis of macrophages for stabilizing vulnerable atherosclerotic plaques, Bioact. Mater. 16 (2022) 120–133.
[81] H. Bruus, Acoustofluidics 7: the acoustic radiation force on small particles, Lab Chip 12 (6) (2012) 1014–1021.
[82] N.S. Awad, et al., Ultrasound-responsive Nanocarriers in Cancer treatment: a review, ACS Pharmacol Transl Sci 4 (2) (2021) 589–612.
[83] A. Giordano, et al., Lipid-based Nanocarriers: bridging diagnosis and Cancer therapy, Pharmaceutics 16 (9) (2024).
[84] J.A. Navarro-Becerra, M.A. Borden, Targeted microbubbles for drug, gene, and cell delivery in therapy and immunotherapy, Pharmaceutics 15 (6) (2023).
[85] S.Y. Lee, et al., A novel liposomal nanomedicine for nitric oxide delivery and breast cancer treatment, Biomed. Mater. Eng. 24 (1) (2014) 61–67.
[86] S.M. Fix, M.A. Borden, P.A. Dayton, Therapeutic gas delivery via microbubbles and liposomes, J. Control. Release 209 (2015) 139–149.
[87] S. Nag, et al., Mechanistic insights into nanobubble merging studied using in situ liquid-phase electron microscopy, Langmuir 37 (2) (2021) 874–881.
[88] N.T. Blum, et al., Nanoparticles formed by acoustic destruction of microbubbles and their utilization for imaging and effects on therapy by high intensity focused ultrasound, Theranostics 7 (3) (2017) 694.
[89] Y.-J. Ho, et al., Normalization of tumor vasculature by oxygen microbubbles with ultrasound, Theranostics 9 (24) (2019) 7370.
[90] Y. Opoku-Damoah, et al., Ultrasound-responsive lipid Nanoplatform with nitric oxide and carbon monoxide release for Cancer Sono-Gaso-therapy, ACS Appl. Bio Mater. 7 (11) (2024) 7585–7594.
[91] Y. Liu, et al., Magnetic nanoliposomes as microbubble bombers for multimodality image-guided cancer theranostics, ACS Nano 11 (2) (2017) 1509–1519.
[92] A. Yildirim, et al., Stable encapsulation of air in mesoporous silica nanoparticles: fluorocarbon-free nanoscale ultrasound contrast agents, Adv. Healthc. Mater. 5 (11) (2016) 1290–1298.
[93] Q. Jin, et al., Roles of textural and surface properties of nanoparticles in ultrasound-responsive systems, Langmuir 34 (4) (2018) 1256–1265.
[94] L. Wang, et al., An ultrasound-triggered nanoplatform for synergistic sonodynamic-nitric oxide therapy, ACS Biomater Sci. Eng. 9 (2) (2023) 797–808.
[95] X. Wang, et al., Perfluorohexane-encapsulated mesoporous silica nanocapsules as enhancement agents for highly efficient high intensity focused ultrasound (HIFU), Adv. Mater. 24 (6) (2012) 785.
[96] K. Zhang, et al., A continuous tri-phase transition effect for HIFU-mediated intravenous drug delivery, Biomaterials 35 (22) (2014) 5875–5885.
[97] P. Wang, et al., Ultrasmall barium Titanate nanoparticles for highly efficient hypoxic tumor therapy via ultrasound triggered Piezocatalysis and water splitting, ACS Nano 15 (7) (2021) 11326–11340.
[98] Q. Zhao, S. Zhong, L. Li, Piezocatalysis for gas generation and disease therapy, Med Gas Res 15 (2) (2025) 202–203.
[99] Y. Wang, et al., Ultrasound-triggered piezocatalysis for selectively controlled NO gas and chemodrug release to enhance drug penetration in pancreatic cancer, ACS Nano 17 (4) (2023) 3557–3573.
[100] Q. Feng, et al., pH/Ultrasound Dual-Responsive Gas Generator for Ultrasound Imaging-Guided Therapeutic Inertial Cavitation and Sonodynamic Therapy, Adv Healthc Mater vol. 7 (5) (2018).
[101] H. Bhardwaj, R.K. Jangde, Current updated review on preparation of polymeric nanoparticles for drug delivery and biomedical applications, Next Nanotechnology 2 (2023) 100013.
[102] R.A. Barmin, et al., Polymeric materials for ultrasound imaging and therapy, Chem. Sci. 14 (43) (2023) 11941–11954.
[103] H.S. Min, et al., Chemical gas-generating nanoparticles for tumor-targeted ultrasound imaging and ultrasound-triggered drug delivery, Biomaterials 108 (2016) 57–70.
[104] H. Yang, et al., Ultrasound-responsive nanoparticles for nitric oxide release to inhibit the growth of breast cancer, Cancer Cell Int. 24 (1) (2024) 434.
[105] B. Wen, et al., Ultrasound-responsive oxygen-carrying pollen for enhancing chemo-Sonodynamic therapy of breast Cancer, Adv Sci (Weinh) 10 (21) (2023) e2300456.
[106] X. Jiang, et al., Gelatin-based anticancer drug delivery nanosystems: a mini review, Front. Bioeng. Biotechnol. 11 (2023) 1158749.
[107] G. Deng, et al., Ferritin in cancer therapy: a pleiotropic tumoraffin nanocage-based transport, Cancer Med. 12 (10) (2023) 11570–11588.
[108] Y. Ishima, Albumin-based nitric oxide traffic system for the treatment of intractable cancers, Biol. Pharm. Bull. 40 (2) (2017) 128–134.
[109] L. Li, et al., Binding and uptake of H-ferritin are mediated by human transferrin receptor-1, Proc. Natl. Acad. Sci. USA 107 (8) (2010) 3505–3510.
[110] Y. Shen, et al., Transferrin receptor 1 in cancer: a new sight for cancer therapy, Am. J. Cancer Res. 8 (6) (2018) 916–931.
[111] K. Li, et al., Size-transformable gelatin/nanochitosan/doxorubicin nanoparticles with sequentially triggered drug release for anticancer therapy, Colloids Surf. B Biointerfaces 220 (2022) 112927.
[112] A.M.J. Coenen, et al., Elastic materials for tissue engineering applications: natural, synthetic, and hybrid polymers, Acta Biomater. 79 (2018) 60–82.
[113] T. Guo, et al., A facile fabrication of core–shell sodium alginate/gelatin beads for drug delivery systems, Polym. Bull. 76 (1) (2019) 87–102.
[114] N. Chang, et al., IR780 loaded perfluorohexane nanodroplets for efficient sonodynamic effect induced by short-pulsed focused ultrasound, Ultrason. Sonochem. 53 (2019) 59–67.
[115] Y. Xu, et al., Damaging tumor vessels with an ultrasound-triggered NO release Nanosystem to enhance drug accumulation and T cells infiltration, Int. J. Nanomedicine 16 (2021) 2597–2613.
[116] L. Song, et al., Biogenic nanobubbles for effective oxygen delivery and enhanced photodynamic therapy of cancer, Acta Biomater. 108 (2020) 313–325.
[117] A. Bar-Zion, et al., Acoustically triggered mechanotherapy using genetically encoded gas vesicles, Nat. Nanotechnol. 16 (12) (2021) 1403–1412.
[118] A. Lakshmanan, et al., Molecular engineering of acoustic protein nanostructures, ACS Nano 10 (8) (2016) 7314–7322.
[119] A. Farhadi, et al., Ultrasound imaging of gene expression in mammalian cells, Science 365 (6460) (2019) 1469–1475.
[120] R.W. Bourdeau, et al., Acoustic reporter genes for noninvasive imaging of microorganisms in mammalian hosts, Nature 553 (7686) (2018) 86–90.
[121] D.P. Sawyer, et al., Ultrasensitive ultrasound imaging of gene expression with signal unmixing, Nat. Methods 18 (8) (2021) 945–952.
[122] A. Farhadi, et al., Recombinantly expressed gas vesicles as nanoscale contrast agents for ultrasound and hyperpolarized MRI, AICHE J. 64 (8) (2018) 2927–2933.
[123] D. Maresca, et al., Acoustic biomolecules enhance hemodynamic functional ultrasound imaging of neural activity, NeuroImage 209 (2020) 116467.
[124] B. Ling, et al., Biomolecular ultrasound imaging of Phagolysosomal function, ACS Nano 14 (9) (2020) 12210–12221.
[125] A. Lakshmanan, et al., Acoustic biosensors for ultrasound imaging of enzyme activity, Nat. Chem. Biol. 16 (9) (2020) 988–996.
[126] P. Dutka, et al., Structure of Anabaena flos-aquae gas vesicles revealed by cryo-ET, Structure 31 (5) (2023) 518–528.e6.
[127] S.T. Huber, et al., Cryo-EM structure of gas vesicles for buoyancy-controlled motility, Cell 186 (5) (2023) 975–986.e13.
[128] M.G. Shapiro, et al., Biogenic gas nanostructures as ultrasonic molecular reporters, Nat. Nanotechnol. 9 (4) (2014) 311–316.
[129] B. Ling, et al., Truly tiny acoustic biomolecules for ultrasound imaging and therapy, Adv. Mater. 36 (28) (2024) e2307106.
[130] J.R. Eisenbrey, et al., Sensitization of hypoxic tumors to radiation therapy using ultrasound-sensitive oxygen microbubbles, Int. J. Radiat. Oncol. Biol. Phys. 101 (1) (2018) 88–96.
[131] C. Zhang, et al., Metal-organic framework (MOF)-based ultrasound-responsive dual-Sonosensitizer Nanoplatform for hypoxic Cancer therapy, Adv. Healthc. Mater. 11 (2) (2022) e2101946.

[132] R. Wu, et al., Ultrasound triggered local sequential reactive oxygen species and nitric oxide release for enhanced cerasomal drug delivery, Chem. Eng. J. 486 (2024) 150134.
[133] S. Sabuncu, A. Yildirim, Gas-stabilizing nanoparticles for ultrasound imaging and therapy of cancer, Nano Converg 8 (1) (2021) 39.
[134] L. Duan, et al., Micro/nano-bubble-assisted ultrasound to enhance the EPR effect and potential theranostic applications, Theranostics 10 (2) (2020) 462.
[135] L. Xu, et al., Lipid nanoparticles for drug delivery, Advanced NanoBiomed Research 2 (2) (2022) 2100109.
[136] Y. Zhao, et al., Ultrasound targeted microbubble destruction-triggered nitric oxide release via nanoscale ultrasound contrast agent for sensitizing chemoimmunotherapy, J. Nanobiotechnol. 21 (1) (2023) 35.
[137] W. Guo, et al., Ultrasound-mediated antitumor therapy via targeted acoustic release carrier of carbon monoxide (TARC-CO), ACS Appl. Mater. Interfaces 14 (45) (2022) 50664–50676.
[138] F. Tang, L. Li, D. Chen, Mesoporous silica nanoparticles: synthesis, biocompatibility and drug delivery, Adv. Mater. 24 (12) (2012) 1504–1534.
[139] T. Asefa, Z. Tao, Biocompatibility of mesoporous silica nanoparticles, Chem. Res. Toxicol. 25 (11) (2012) 2265–2284.
[140] A.E. Nel, et al., Understanding biophysicochemical interactions at the nano–bio interface, Nat. Mater. 8 (7) (2009) 543–557.
[141] N. Khlebtsov, L. Dykman, Biodistribution and toxicity of gold nanoparticles, Nanotechnologies in Russia 6 (1) (2011) 17–42.
[142] S.M. Moghimi, et al., Material properties in complement activation, Adv. Drug Deliv. Rev. 63 (12) (2011) 1000–1007.
[143] T. Zhang, et al., CoOx-caged metal-organic frameworks for Sonocatalyzing CO2 to CO for ultrasound-assisted Chemodynamic-gas Cancer therapy, Adv. Funct. Mater. 34 (8) (2024) 2311029.
[144] J. Zhu, et al., An ultrasound activated cyanine-rhenium (I) complex for sonodynamic and gas synergistic therapy, Chem. Commun. 58 (20) (2022) 3314–3317.
[145] T.M. Allen, P.R. Cullis, Drug delivery systems: entering the mainstream, Science 303 (5665) (2004) 1818–1822.
[146] S. Mura, J. Nicolas, P. Couvreur, Stimuli-responsive nanocarriers for drug delivery, Nat. Mater. 12 (11) (2013) 991–1003.
[147] H.S. Min, et al., Chemical gas-generating nanoparticles for tumor-targeted ultrasound imaging and ultrasound-triggered drug delivery, Biomaterials 108 (2016) 57–70.
[148] B. Wen, et al., Ultrasound-responsive oxygen-carrying pollen for enhancing chemo-sonodynamic therapy of breast cancer, Adv. Sci. 10 (21) (2023) 2300456.
[149] H. Yang, et al., Ultrasound-responsive nanoparticles for nitric oxide release to inhibit the growth of breast cancer, Cancer Cell Int. 24 (1) (2024) 434.
[150] B. Leader, Q.J. Baca, D.E. Golan, Protein therapeutics: a summary and pharmacological classification, Nat. Rev. Drug Discov. 7 (1) (2008) 21–39.
[151] F.M. Wurm, Production of recombinant protein therapeutics in cultivated mammalian cells, Nat. Biotechnol. 22 (11) (2004) 1393–1398.
[152] A.S. De Groot, D.W. Scott, Immunogenicity of protein therapeutics, Trends Immunol. 28 (11) (2007) 482–490.
[153] N. Chang, et al., IR780 loaded perfluorohexane nanodroplets for efficient sonodynamic effect induced by short-pulsed focused ultrasound, Ultrason. Sonochem. 53 (2019) 59–67.
[154] Y. Xu, et al., Damaging tumor vessels with an ultrasound-triggered NO release nanosystem to enhance drug accumulation and T cells infiltration, Int. J. Nanomedicine (2021) 2597–2613.
[155] B. Ling, et al., Truly tiny acoustic biomolecules for ultrasound imaging and therapy, Adv. Mater. 36 (28) (2024) 2307106.
[156] J. Shi, et al., Cancer nanomedicine: progress, challenges and opportunities, Nat. Rev. Cancer 17 (1) (2017) 20–37.
[157] D. Bobo, et al., Nanoparticle-based medicines: a review of FDA-approved materials and clinical trials to date, Pharm. Res. 33 (10) (2016) 2373–2387.
[158] J.R. Eisenbrey, et al., Sensitization of hypoxic tumors to radiation therapy using ultrasound-sensitive oxygen microbubbles. International journal of radiation oncology* biology*, Physics 101 (1) (2018) 88–96.
[159] T. Yin, et al., Hypoxia-alleviated sonodynamic therapy based on a hybrid protein oxygen carrier to enhance tumor inhibition, Biomater. Sci. 10 (1) (2022) 294–305.
[160] X. Liu, et al., Magnetic resonance imaging Nanoprobe quantifies nitric oxide for evaluating M1/M2 macrophage polarization and prognosis of Cancer treatments, ACS Nano 17 (24) (2023) 24854–24866.
[161] Z. Jiang, et al., A NIR-II photoacoustic probe for high spatial quantitative imaging of tumor nitric oxide in vivo, Angew. Chem. Int. Ed. Engl. 63 (19) (2024) e202320072.
[162] Y.D. Zhao, et al., Ultrasound targeted microbubble destruction-triggered nitric oxide release via nanoscale ultrasound contrast agent for sensitizing chemoimmunotherapy, J. Nanobiotechnol. 21 (1) (2023).
[163] W.Q. Zhang, et al., Characterising the chemical and physical properties of phase-change nanodroplets, Ultrason. Sonochem. 97 (2023).
[164] J. Tu, et al., Ultrasound-mediated microbubble destruction: a new method in cancer immunotherapy, Onco. Targets. Ther. 11 (2018) 5763–5775.
[165] T. Saliev, M. Akishev, Ultrasound binary microbubble drug delivery and drug synthesis for cancer treatment. Journal of analytical, Sci. Technol. 16 (1) (2025).
[166] L.M. Thomson, et al., Manufacture of concentrated, lipid-based oxygen microbubble emulsions by high shear homogenization and serial concentration, JoVE 87 (2014) e51467.
[167] R. Paliwal, R.J. Babu, S. Palakurthi, Nanomedicine scale-up technologies: feasibilities and challenges, AAPS PharmSciTech 15 (6) (2014) 1527–1534.
[168] N. Seegobin, et al., Optimising the production of PLGA nanoparticles by combining design of experiment and machine learning, Int. J. Pharm. 667 (2024) 124905.
[169] S. Al-Jawadi, S.S. Thakur, Ultrasound-responsive lipid microbubbles for drug delivery: a review of preparation techniques to optimise formulation size, stability and drug loading, Int. J. Pharm. 585 (2020) 119559.
[170] S. Gimondi, et al., Microfluidic devices: a tool for nanoparticle synthesis and performance evaluation, ACS Nano 17 (15) (2023) 14205–14228.
[171] T.L. Moore, et al., Unleashing the power of machine learning in nanomedicine formulation development, Adv. Funct. Mater. (2025) e14387, https://doi.org/10.1002/adfm.202514387.
[172] N. McDannold, N. Vykhodtseva, K. Hynynen, Targeted disruption of the blood-brain barrier with focused ultrasound: association with cavitation activity, Phys. Med. Biol. 51 (4) (2006) 793–807.
[173] L.J. Delaney, et al., Making waves: how ultrasound-targeted drug delivery is changing pharmaceutical approaches, Materials Advances 3 (7) (2022) 3023–3040.
[174] B. Helfield, Y.R. Zou, N. Matsuura, Acoustically-Stimulated Nanobubbles: Opportunities in Medical Ultrasound Imaging and Therapy, Frontiers in Physics 9 (2021).
[175] T. Gatica, R. Haqshenas, Classifying acoustic cavitation with machine learning trained on multiple physical models, Phys. Fluids 37 (3) (2025).
[176] N. Lamothe, et al., Monitoring holograms for therapeutic ultrasound using passive cavitation beamforming, Appl. Acoust. 224 (2024) 110144.
[177] M. Sivasubramanian, et al., Personalized cancer therapeutics using photoacoustic imaging-guided sonodynamic therapy, IEEE Trans. Ultrason. Ferroelectr. Freq. Control 70 (12) (2023) 1682–1690.
[178] S. Hernot, A.L. Klibanov, Microbubbles in ultrasound-triggered drug and gene delivery, Adv. Drug Deliv. Rev. 60 (10) (2008) 1153–1166.
[179] A.H. Khan, et al., Combining ultrasound and capillary-embedded T-junction microfluidic devices to scale up the production of narrow-sized microbubbles through acoustic fragmentation, Langmuir 38 (33) (2022) 10288–10304.
[180] N.L. Hunter, R.E. Sherman, Combination products: modernizing the regulatory paradigm, Nat. Rev. Drug Discov. 16 (8) (2017) 513–514.
[181] J. Schwartz, C. Macomber, So, you think you have an idea: a practical risk reduction-conceptual model for academic translational research, Bioengineering (Basel) 4 (2) (2017).
[182] Q.Y. Hu, et al., Progress and preclinical application status of ultrasound microbubbles, J. Drug Delivery Sci. Technol. 92 (2024).
[183] D. Moore-Palhares, et al., Radiation enhancement using focussed ultrasound-stimulated microbubbles for breast cancer: a phase 1 clinical trial, PLoS Med. 21 (5) (2024) e1004408.
[184] G. Pasqual-Melo, et al., Combination of gas plasma and radiotherapy has Immunostimulatory potential and additive toxicity in murine melanoma cells in vitro, Int. J. Mol. Sci. 21 (4) (2020).
[185] L. Yu, et al., Gas plasma combination therapies-promises from preclinical oncology research, Antioxidants (Basel) 14 (9) (2025).
[186] M. Chen, et al., A gas Nanobomb to promote drug penetration and amplify TACE therapy for Orthotopic liver tumor, Adv. Mater. 37 (39) (2025) e2505770.
[187] S. Mullick Chowdhury, T. Lee, J.K. Willmann, Ultrasound-guided drug delivery in cancer, Ultrasonography 36 (3) (2017) 171–184.
[188] L. Fang, et al., Ultrasound-responsive lipid Nanosonosensitizers with size reduction and NO release: synergistic Sonodynamic-chemo-immunotherapy for pancreatic tumors, Angew. Chem. Int. Ed. 64 (2025) e202507388, https://doi.org/10.1002/anie.202507388.
[189] Y. Song, et al., Ultrasound-mediated Piezocatalysis triggers NO release to augment targeted immunotherapy of pancreatic Cancer, ACS Nano 19 (36) (2025) 32654–32673.
[190] Q. Gao, et al., Stimuli-responsive TiCT MXene-based hydrogels: preparation and applications, Materials Chemistry Frontiers 8 (9) (2024) 2056–2077.
[191] R. Liu, et al., Near-infrared light-triggered nano-prodrug for cancer gas therapy, J. Nanobiotechnol. 19 (1) (2021) 443.